Electronic Supplementary Information

Trace Amount Cu^{II}(ppm) and Mixture Design of Cu^{II}/Pd^{II} Catalyzed Suzuki Cross-Coupling Reactions Based on Cooperative Interaction of Metal with a Conjugated Pyridylspirobifluorene

Xing Li,*[a] Jie Zhang,[a,b] Yayun Zhao,[a] Xiuhua Zhao,[a] Feng Li,[b] Taohai Li,*[b] H. L. Li[c] and Liang Chen[c]

[a] State Key Laboratory Base of Novel Functional Materials and Preparation Science, Faculty of Materials Science and Chemical Engineering, Ningbo University, Ningbo, 315211, P.R. China

[b] College of Chemistry, Xiangtan University, Xiangtan 411105, P.R. China

[c] Ningbo Institute of Materials Technology and Engineering, Zhejiang, Ningbo, 315211, P.R. China

* Corresponding author E-mail addresses: lixing@nbu.edu.cn

EXPERIMENTAL SECTION

Materials and Methods. All catalysis coupling reactions were carried out under air atmosphere. All other synthetic reactions were performed by using standard Schlenk techniques utilizing a double-manifold vacuum system with high purity nitrogen flow. Poly(ethylenimine) (abbreviated as PEI) was purchased from Aldrich Chemical Company. All solutions were prepared with doubly-distilled water. All reagents were of analytical grade and used as received without further purification.

Physical Measurements. Infra-red spectra were recorded on a Nicolet Avatar FTIR spectrophotometer in the range 4000-400 cm^{-1}. NMR spectra were obtained from solutions in $CDCl_3$ using Bruker DRX-400 spectrometers. Gas chromatography-mass spectrometry (GC-MS) was performed on a 430 GC (Varian, USA). UV–vis absorption spectra were recorded on a quartz slide using a Lambda35 spectrophotometer (Perkin Elmer, USA). Atomic force microscope (AFM) images were taken on a single-crystal silicon slide using a Veeco Multimode NS3A-02NanoscopeIII atomic force microscope with silicon tips. Height images of the films were recorded using tapping-mode AFM. Analysis of Pd content was measured by inductively coupled plasma-atomic emission spectroscopy (ICP-AES) using Ultima. Transmission electron microscopy (TEM) images were obtained by Tecnai G2 F20 S-TWIN. Scanning electron microscopy (SEM) images were taken with SU-70 field-emission scanning electron microscope. Energy dispersive X-ray spectra (EDS) were carried out on a Carl Zeiss model Ultra 55 microscope. Powder X-ray diffraction (PXRD) data were collected on a Bruker D8 Focus X-ray diffractometer using Cu Kα radiation.

Synthesis the complex of 2,2′,7,7′-tetra-(4-pyridyl)-9,9′-spirobifluorene. A mixture of 2,2′,7,7′-tetrabromo-9,9′-spirobifluorene (1.5 mmol), pyridine-4-boronic acid (9.0 mmol), K_2CO_3 (30 mmol), $Pd(PPh_3)_4$ (0.15 mmol) were dissolved in toluene/EtOH/H_2O (80/40/20 mL). The mixture was refluxed under N_2 for 48 h, cooled to the room temperature, and then extracted with CH_2Cl_2. The combined organic phase was dried with anhydrous $MgSO_4$, and concentrated by evaporation under reduced pressure. The obtained sample was purified by column chromatography. The psf was obtained, yield 75%. Recrystallized from CH_2Cl_2 / DMF. ^1H NMR ($CDCl_3$, 400 MHz): 8.533-8.547 (d, 8H, -C_5H_4N), 8.061-8.081 (d, 4H, -C_6H_3), 7.780-7.760 (d, 4H, -C_6H_3), 7.365-7.380 (d, 8H, -C_5H_4N), 7.066ppm (s, 4H, -C_6H_3); ^{13}C NMR ($CDCl_3$, 100 MHz): δ = 150.01(C),

149.50(C), 147.68(C), 141.96(C), 138.52(C), 127.54(CH), 122.54(CH), 121.46(CH), 121.37(CH), 66.15(C_{spiro}) ppm. MS (ESI): m/z calcd for $C_{45}H_{28}N_4$: 624.4; found 625.4 ($M + H^+$).

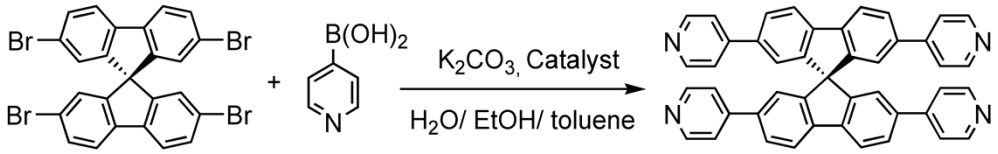

Scheme S1**. Synthesis schematic diagram of the psf ligand.**

X-ray Crystallography. Data collection for psf was performed on a Bruker-AXS diffractometer equipped with a graphite monochromated Mo-Kα radiation (λ = 0.71073 Å) at 293K. All absorption corrections were applied using the SADABS program. The structure was solved by direct methods, the metal atom was located from the E-map, and other non-hydrogen atoms were derived from the successive difference Fourier syntheses. All non-hydrogen atoms were refined anisotropically, while the hydrogen atoms were generated geometrically and refined with isotropic thermal parameters. The structure was refined on F^2 by full-matrix least-squares using the SHELXTL-97 program package. The crystallographic data of psf were listed in Table S1 and the selected bond lengths and angles in Table S2. Crystallographic data (excluding structure factors) for psf have been deposited at the Cambridge Crystallographic Data Center as supplementary publications. CCDC-982005 for the psf ligand contains the crystallographic data. The data can be obtained free of charge at www.ccdc.cam.ac.uk/conts/retrieving.html [or from the Cam-bridge Crystallographic Data Centre, 12, Union Road, Cambridge CB2 1EZ, UK; E-mail: deposit@ccdc.cam.ac.uk].

Preparation of Combination (Pd/psf) Nanoparticles. The ethanol solution of psf (5.0 mmol/L, 1.0 mL) was added to aqueous solution of $PdCl_2$ (5.0 mmol/L, 1.0 mL), then the mixture was stirred at 90 ºC for 10h until a pale yellow suspension was obtained. The suspension was centrifuged, washed with water and ethanol, dried for SEM. The size of the nanoparticles was determined by SEM.

Preparation of Combination (Cu/psf) Sheets. A mixture of $Cu(NO_3)_2{\cdot}6H_2O$ (0.03mmol), psf (0.03mmol), EtOH (1.0 mL) and H_2O (1.0 mL) was stirred for appropriate time under ambient atmosphere. $Cu(NO_3)_2$/psf nanoparticles were prepared, separated, washed three times with water and ethanol, and dried in the air for SEM. The size of the sheets was determined by SEM.

Preparation of Combination (Cu/Pd/psf) Composites. A mixture of $Cu(NO_3)_2 \cdot 6H_2O$ (0.15mmol), $PdCl_2$ (0.15mmol), psf (0.03mmol), EtOH (1.0 mL) and H_2O (1.0 mL) was stirred for 10h under ambient atmosphere, and then blue colloidal suspension was obtained, separated, washed with water and ethanol, and dried in the air for SEM.

Layer-by-Layer Assembly of Multilayer Films. The quartz sheets were treated with a mixture solution (H_2SO_4 / 30 % H_2O_2 = 6:4; Caution: this solution is an extremely dangerous corrosive and should be handled with care using appropriate personal protection) at 70ºC for 30min, followed by thoroughly washing with distilled water and drying under nitrogen flow. Further purification was carried out by immersion in a H_2O / H_2O_2 / NH_4OH (5:1:1) (V/V/V) bath for 30 min at 70 ºC. The clean quartz sheets were first immersed in PEI solution for 10 min. Then the sheets were deposited into $Cu(NO_3)_2$ solution (3.0 mmol / L) for 10 min. The sheets coated with PEI-Cu^{2+} were immersed in the ethanol solution of the psf for 10 min. By repeating the steps above, PEI-$[Cu(NO_3)_2/psf]_n$ multilayer films were prepared. Between each immersion step, the substrates were dried with nitrogen stream at room temperature.

Analysis of Cu-loadings in PEI-$[Cu(NO_3)_2/psf]_{10}$ Film. The amount of copper in the PEI-$[Cu(NO_3)_2/psf]_{10}$ was determined as follows: the quartz sheet loaded with PEI-$[Cu(NO_3)_2/psf]_{10}$ was put into a NaOH aqueous solution (0.5 mM, 10 mL), and UV-vis spectra were used to monitor the absorbance; when the quartz sheet exhibited no absorbance, indicating the PEI-$(Cu^{2+}/psf)_{10}$ film was completely desorbed into the aqueous solution, and the solution was used for analysis of Cu-content by ICP (8.7μg, 1.4×10^{-5} mol%).

Application of Catalysts for Suzuki Reaction. The Suzuki cross-coupling reaction was performed by using the slide coated with PEI-$[Cu(NO_3)_2/psf]_n$ multilayer films as catalysts, in which the coated slide was submerged to the reaction mixture in a small pressure-proof vial with a magnetic bar (Scheme 2). In this reaction, the general procedure was as follows: the mixture of aryl boronic acid or its derivative (1.2 mmol), aryl halide (1.0 mmol), K_2CO_3 (3.0 mmol), catalyst H_2O and EtOH and was put into a vial. Then the mixture was heated to an appropriate temperature for a certain time with vigorously stirring. At the end of the reaction, the mixture was cooled and extracted with ethyl acetate (10 mL) for three times. The organic phase was collected, washed with saturated brine and dried by anhydrous sodium sulfate.

After removal of the solvent, the residue was purified by column chromatography on silica gel. ^{1}H NMR (400 MHz) and ^{13}C NMR (100 MHz) spectra were recorded in $CDCl_3$ solution (SM).

IR, MS, ^{1}H NMR, ^{13}C NMR of the psf ligand.

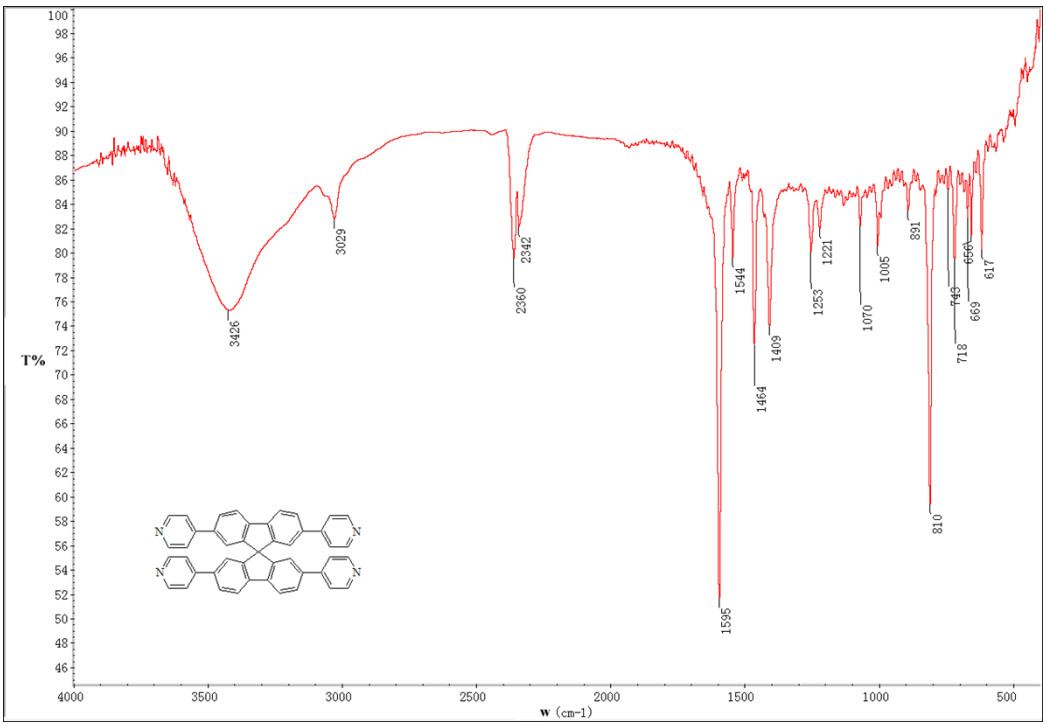

Fig. S1. FTIR spectrum of the psf ligand

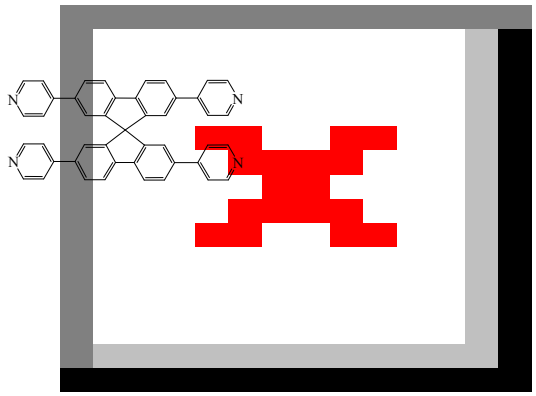

Fig. S2. Mass spectrogram of the psf ligand

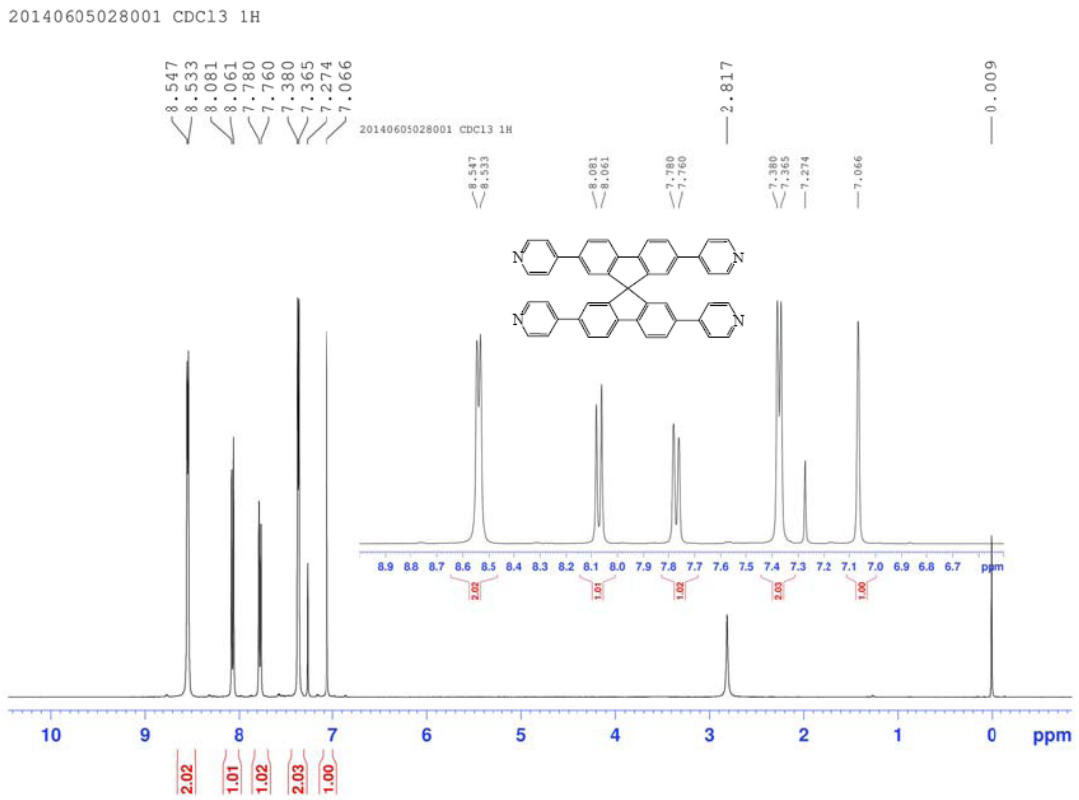

Fig. S3. ^{1}H NMR spectrum of the psf ligand.

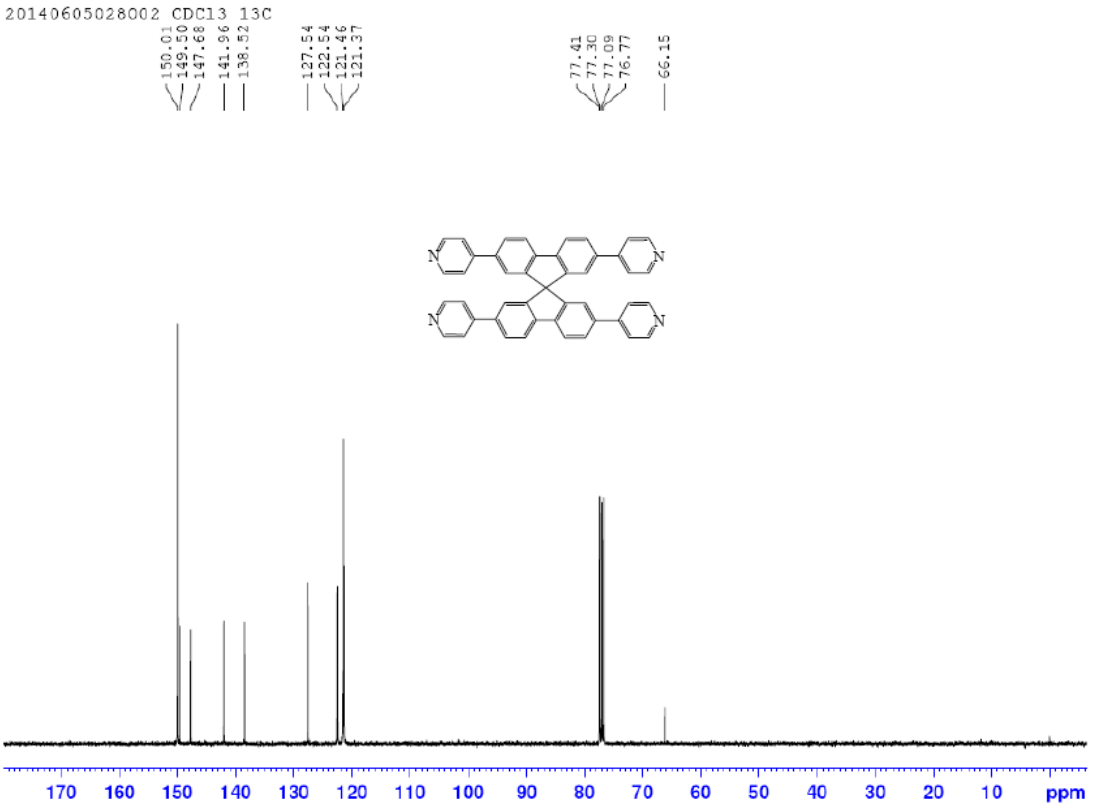

Fig. S4. ^{13}C NMR spectrum of the psf ligand.

Table S1. Crystal data and structure refinement for psf.

Identification code	psf·$(H_2O)_5(CH_3OH)_4$	
Empirical formula	$C_{94}H_{82}N_8O_9$	
Formula weight	1467.70	
Temperature (K)	293(2)	
Wavelength (Å)	0.71073	
Crystal system	Triclinic	
space group	*P*-1	
Unit cell dimensions	a = 14.285(9) Å	α = 69.009(9) º
	b = 15.991(10) Å	β = 71.138(8) º
	c = 20.393(12) Å	γ = 88.044(9) º
Volume (Å^3)	4098(4)	
Z	2	
Calculated density (Mg/m^3)	1.168	
Absorption coefficient (mm^{-1})	0.076	
F(000)	1496	
Crystal size (mm)	0.24 x 0.12 x 0.08	
Theta range for data collection (º)	1.42 to 27.33	
Limiting indices	-18<=h<=17, -20<=k<=20, -26<=l<=25	
Reflections collected / unique	35481 / 18001 [$R_{(int)}$ = 0.0930]	
Completeness to theta = 27.33	97.3 %	
Max. and min. transmission	0.9939 and 0.9819	
Refinement method	Full-matrix least-squares on F^2	
Data / restraints / parameters	18001 / 0 / 2	
Goodness-of-fit on F^2	0.939	
Final R indices [$I > 2\sigma(I)$]	R_1 = 0.1108, wR_2 = 0.2906	
R indices (all data)	R_1 = 0.2907, wR_2 = 0.3963	
Extinction coefficient	0.0070(12)	
Largest diff. peak and hole (e. Å^{-3})	0.914 and -0.270	

Table S2. Selected bond lengths [Å] and angles [°] for psf.

O(1)-O(3)#1	1.5605	O(1)-C(91)	1.7673	O(2)-C(92)	1.5958
O(2)-O(6)#2	1.7432	O(3)-O(1)#1	1.5605	O(3)-C(93)	1.6905
O(4)-C(94)	1.3750	O(4)-O(9)#3	1.5555	O(5)-C(94)#4	1.4779
O(6)-O(2)#5	1.7432	O(7)-C(94)#6	1.1633	O(8)-O(9)#3	1.3742
O(9)-O(8)#3	1.3742	O(9)-O(4)#3	1.5555	N(1)-C(1)	1.3296
N(1)-C(3)	1.3409	N(2)-C(18)	1.2918	N(2)-C(19)	1.3359
N(3)-C(30)	1.3172	N(3)-C(29)	1.3192	N(4)-C(41)	1.3297
N(4)-C(42)	1.3388	N(5)-C(46)	1.3507	N(5)-C(48)	1.3587
N(6)-C(64)	1.3297	N(6)-C(63)	1.3581	N(7)-C(75)	1.3114

N(7)-C(74)	1.3261	N(8)-C(87)	1.3322	N(8)-C(86)	1.3338
C(1)-C(2)	1.3821	C(2)-C(5)	1.3948	C(3)-C(4)	1.3980
C(4)-C(5)	1.4030	C(5)-C(6)	1.4770	C(6)-C(7)	1.3825
C(6)-C(9)	1.4134	C(7)-C(8)	1.3833	C(8)-C(11)	1.3766
C(9)-C(10)	1.3912	C(10)-C(11)	1.3964	C(10)-C(23)	1.5372
C(11)-C(12)	1.4787	C(12)-C(13)	1.3953	C(12)-C(22)	1.3956
C(13)-C(14)	1.3811	C(14)-C(15)	1.4060	C(15)-C(21)	1.4126
C(15)-C(16)	1.4807	C(16)-C(20)	1.3673	C(16)-C(17)	1.3940
C(17)-C(18)	1.4054	C(19)-C(20)	1.3908	C(21)-C(22)	1.3690
C(22)-C(23)	1.5399	C(23)-C(45)	1.5267	C(23)-C(24)	1.5327
C(24)-C(34)	1.3880	C(24)-C(25)	1.3892	C(25)-C(26)	1.4024
C(26)-C(32)	1.3922	C(26)-C(27)	1.5087	C(27)-C(28)	1.3869
C(27)-C(31)	1.4087	C(28)-C(29)	1.3665	C(30)-C(31)	1.3630
C(32)-C(33)	1.3746	C(33)-C(34)	1.3946	C(34)-C(35)	1.4826
C(35)-C(36)	1.3839	C(35)-C(45)	1.4268	C(36)-C(37)	1.3616
C(37)-C(38)	1.4099	C(38)-C(44)	1.4055	C(38)-C(39)	1.4887
C(39)-C(40)	1.3835	C(39)-C(43)	1.4069	C(40)-C(41)	1.3560
C(42)-C(43)	1.3720	C(44)-C(45)	1.3712	C(46)-C(47)	1.3454
C(47)-C(50)	1.3932	C(48)-C(49)	1.3605	C(49)-C(50)	1.4267
C(50)-C(51)	1.4837	C(51)-C(52)	1.3914	C(51)-C(54)	1.4197
C(52)-C(53)	1.3847	C(53)-C(56)	1.3810	C(54)-C(55)	1.3743
C(55)-C(56)	1.3956	C(55)-C(68)	1.5409	C(56)-C(57)	1.4676
C(57)-C(58)	1.3933	C(57)-C(67)	1.4008	C(58)-C(59)	1.3915
C(59)-C(60)	1.4168	C(60)-C(66)	1.3979	C(60)-C(61)	1.4666
C(61)-C(65)	1.3474	C(61)-C(62)	1.3920	C(62)-C(63)	1.3600
C(64)-C(65)	1.3951	C(66)-C(67)	1.3900	C(67)-C(68)	1.5319
C(68)-C(90)	1.5309	C(68)-C(69)	1.5383	C(69)-C(70)	1.3835
C(69)-C(79)	1.3913	C(70)-C(71)	1.4254	C(71)-C(77)	1.3979
C(71)-C(72)	1.4570	C(72)-C(76)	1.3907	C(72)-C(73)	1.3957
C(73)-C(74)	1.3891	C(75)-C(76)	1.4136	C(77)-C(78)	1.4018
C(78)-C(79)	1.3791	C(79)-C(80)	1.4698	C(80)-C(81)	1.3903
C(80)-C(90)	1.4095	C(81)-C(82)	1.3714	C(82)-C(83)	1.3883
C(83)-C(89)	1.4148	C(83)-C(84)	1.5113	C(84)-C(85)	1.3763
C(84)-C(88)	1.3974	C(85)-C(86)	1.3724	C(87)-C(88)	1.3836
C(89)-C(90)	1.3777	C(94)-O(7)#6	1.1633	C(94)-O(5)#4	1.4779
O(3)#1-O(1)-C(91)	128.9	C(92)-O(2)-O(6)#2	110.4	O(1)#1-O(3)-C(93)	96.6
C(94)-O(4)-O(9)#3	126.4	O(8)#3-O(9)-O(4)#3	117.1	C(1)-N(1)-C(3)	115.8
C(18)-N(2)-C(19)	115.3	C(30)-N(3)-C(29)	114.8	C(41)-N(4)-C(42)	115.0
C(46)-N(5)-C(48)	115.6	C(64)-N(6)-C(63)	114.0	C(75)-N(7)-C(74)	115.9
C(87)-N(8)-C(86)	116.3	N(1)-C(1)-C(2)	124.5	C(1)-C(2)-C(5)	119.8
N(1)-C(3)-C(4)	124.6	C(3)-C(4)-C(5)	118.5	C(2)-C(5)-C(4)	116.8
C(2)-C(5)-C(6)	121.1	C(4)-C(5)-C(6)	122.0	C(7)-C(6)-C(9)	118.4
C(7)-C(6)-C(5)	120.6	C(9)-C(6)-C(5)	121.0	C(6)-C(7)-C(8)	122.3
C(11)-C(8)-C(7)	119.2	C(10)-C(9)-C(6)	119.4	C(9)-C(10)-C(11)	120.5
C(9)-C(10)-C(23)	129.0	C(11)-C(10)-C(23)	110.4	C(8)-C(11)-C(10)	120.2
C(8)-C(11)-C(12)	131.3	C(10)-C(11)-C(12)	108.5	C(13)-C(12)-C(22)	119.7
C(13)-C(12)-C(11)	131.3	C(22)-C(12)-C(11)	108.8	C(14)-C(13)-C(12)	118.7
C(13)-C(14)-C(15)	122.7	C(14)-C(15)-C(21)	116.9	C(14)-C(15)-C(16)	121.1
C(21)-C(15)-C(16)	121.7	C(20)-C(16)-C(17)	115.6	C(20)-C(16)-C(15)	121.6

C(17)-C(16)-C(15)	122.8	C(16)-C(17)-C(18)	120.3	N(2)-C(18)-C(17)	124.0
N(2)-C(19)-C(20)	125.4	C(16)-C(20)-C(19)	119.3	C(22)-C(21)-C(15)	120.7
C(21)-C(22)-C(12)	121.1	C(21)-C(22)-C(23)	128.7	C(12)-C(22)-C(23)	110.2
C(45)-C(23)-C(24)	102.1	C(45)-C(23)-C(10)	118.8	C(24)-C(23)-C(10)	109.5
C(45)-C(23)-C(22)	113.0	C(24)-C(23)-C(22)	112.9	C(10)-C(23)-C(22)	100.9
C(34)-C(24)-C(25)	121.7	C(34)-C(24)-C(23)	111.1	C(25)-C(24)-C(23)	127.1
C(24)-C(25)-C(26)	118.3	C(32)-C(26)-C(25)	118.7	C(32)-C(26)-C(27)	121.7
C(25)-C(26)-C(27)	119.6	C(28)-C(27)-C(31)	114.9	C(28)-C(27)-C(26)	122.9
C(31)-C(27)-C(26)	122.1	C(29)-C(28)-C(27)	120.1	N(3)-C(29)-C(28)	125.2
N(3)-C(30)-C(31)	125.6	C(30)-C(31)-C(27)	119.4	C(33)-C(32)-C(26)	123.4
C(32)-C(33)-C(34)	117.5	C(24)-C(34)-C(33)	120.3	C(24)-C(34)-C(35)	108.8
C(33)-C(34)-C(35)	130.9	C(36)-C(35)-C(45)	118.9	C(36)-C(35)-C(34)	132.7
C(45)-C(35)-C(34)	108.4	C(37)-C(36)-C(35)	120.5	C(36)-C(37)-C(38)	121.3
C(44)-C(38)-C(37)	118.9	C(44)-C(38)-C(39)	120.0	C(37)-C(38)-C(39)	121.1
C(40)-C(39)-C(43)	115.5	C(40)-C(39)-C(38)	122.8	C(43)-C(39)-C(38)	121.7
C(41)-C(40)-C(39)	120.5	N(4)-C(41)-C(40)	125.1	N(4)-C(42)-C(43)	124.6
C(42)-C(43)-C(39)	119.3	C(45)-C(44)-C(38)	119.6	C(44)-C(45)-C(35)	120.7
C(44)-C(45)-C(23)	129.4	C(35)-C(45)-C(23)	109.7	C(47)-C(46)-N(5)	124.6
C(46)-C(47)-C(50)	120.6	N(5)-C(48)-C(49)	123.9	C(48)-C(49)-C(50)	119.5
C(47)-C(50)-C(49)	115.8	C(47)-C(50)-C(51)	121.8	C(49)-C(50)-C(51)	122.4
C(52)-C(51)-C(54)	117.7	C(52)-C(51)-C(50)	120.9	C(54)-C(51)-C(50)	121.3
C(53)-C(52)-C(51)	122.3	C(56)-C(53)-C(52)	119.1	C(55)-C(54)-C(51)	119.9
C(54)-C(55)-C(56)	120.9	C(54)-C(55)-C(68)	128.1	C(56)-C(55)-C(68)	111.0
C(53)-C(56)-C(55)	120.0	C(53)-C(56)-C(57)	131.5	C(55)-C(56)-C(57)	108.5
C(58)-C(57)-C(67)	120.4	C(58)-C(57)-C(56)	130.6	C(67)-C(57)-C(56)	108.9
C(59)-C(58)-C(57)	118.1	C(58)-C(59)-C(60)	122.7	C(66)-C(60)-C(59)	117.6
C(66)-C(60)-C(61)	121.6	C(59)-C(60)-C(61)	120.7	C(65)-C(61)-C(62)	116.0
C(65)-C(61)-C(60)	121.7	C(62)-C(61)-C(60)	122.3	C(63)-C(62)-C(61)	121.1
N(6)-C(63)-C(62)	123.8	N(6)-C(64)-C(65)	125.1	C(61)-C(65)-C(64)	120.0
C(67)-C(66)-C(60)	120.4	C(66)-C(67)-C(57)	120.8	C(66)-C(67)-C(68)	128.4
C(57)-C(67)-C(68)	110.8	C(90)-C(68)-C(67)	117.3	C(90)-C(68)-C(69)	101.7
C(67)-C(68)-C(69)	114.2	C(90)-C(68)-C(55)	109.9	C(67)-C(68)-C(55)	100.7
C(69)-C(68)-C(55)	113.6	C(70)-C(69)-C(79)	120.8	C(70)-C(69)-C(68)	128.5
C(79)-C(69)-C(68)	110.7	C(69)-C(70)-C(71)	119.8	C(77)-C(71)-C(70)	118.1
C(77)-C(71)-C(72)	120.5	C(70)-C(71)-C(72)	121.5	C(76)-C(72)-C(73)	116.6
C(76)-C(72)-C(71)	121.4	C(73)-C(72)-C(71)	122.0	C(74)-C(73)-C(72)	119.2
N(7)-C(74)-C(73)	124.9	N(7)-C(75)-C(76)	124.6	C(72)-C(76)-C(75)	118.7
C(71)-C(77)-C(78)	121.3	C(79)-C(78)-C(77)	119.5	C(78)-C(79)-C(69)	120.4
C(78)-C(79)-C(80)	131.1	C(69)-C(79)-C(80)	108.4	C(81)-C(80)-C(90)	119.2
C(81)-C(80)-C(79)	131.3	C(90)-C(80)-C(79)	109.5	C(82)-C(81)-C(80)	120.4
C(81)-C(82)-C(83)	120.8	C(82)-C(83)-C(89)	119.9	C(82)-C(83)-C(84)	119.5
C(89)-C(83)-C(84)	120.6	C(85)-C(84)-C(88)	117.3	C(85)-C(84)-C(83)	120.1
C(88)-C(84)-C(83)	122.6	C(86)-C(85)-C(84)	119.5	N(8)-C(86)-C(85)	124.2
N(8)-C(87)-C(88)	123.7	C(87)-C(88)-C(84)	118.9	C(90)-C(89)-C(83)	118.9
C(89)-C(90)-C(80)	120.9	C(89)-C(90)-C(68)	129.5	C(80)-C(90)-C(68)	109.4
O(7)#6-C(94)-O(4)	120.1	O(7)#6-C(94)-O(5)#4	126.6	O(4)-C(94)-O(5)#4	113.3

Symmetry transformations used to generate equivalent atoms: #1 -x+2,-y+1,-z+1; #2 x,y-1,z+1; #3 -x+2,-y,-z+1; #4 -x+1,-y+1,-z; #5 x,y+1,z-1; #6 -x+2,-y+1,-z

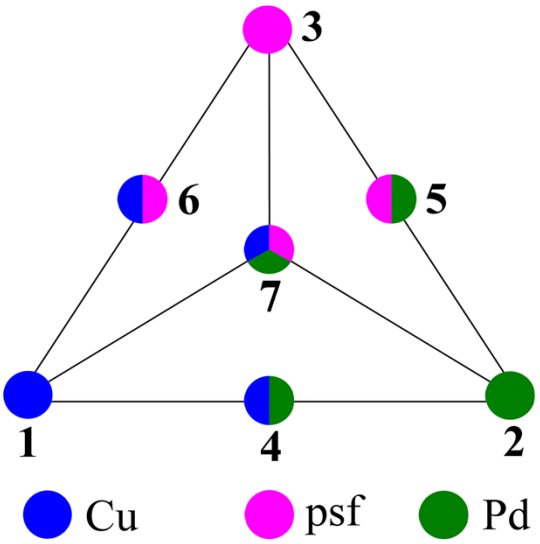

Fig. S5. Mixture designs of copper, palladium and psf.

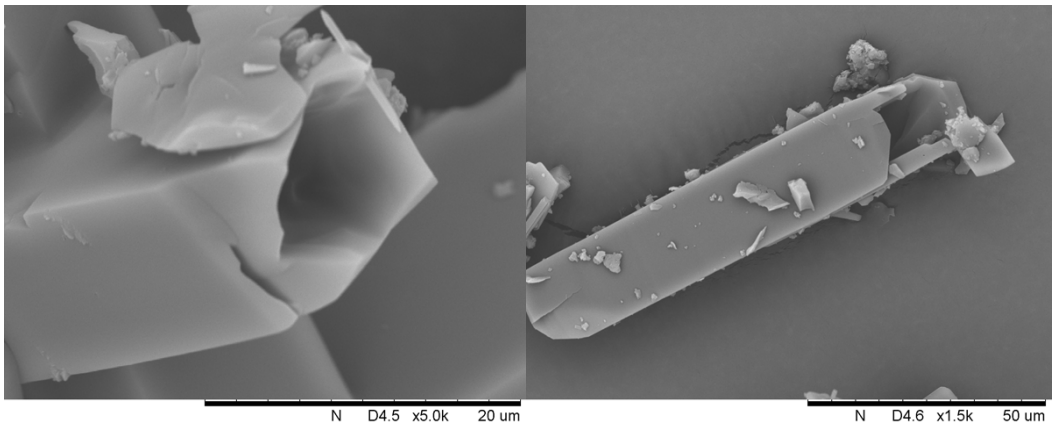

Fig. S6. SEM views of the psf ligand.

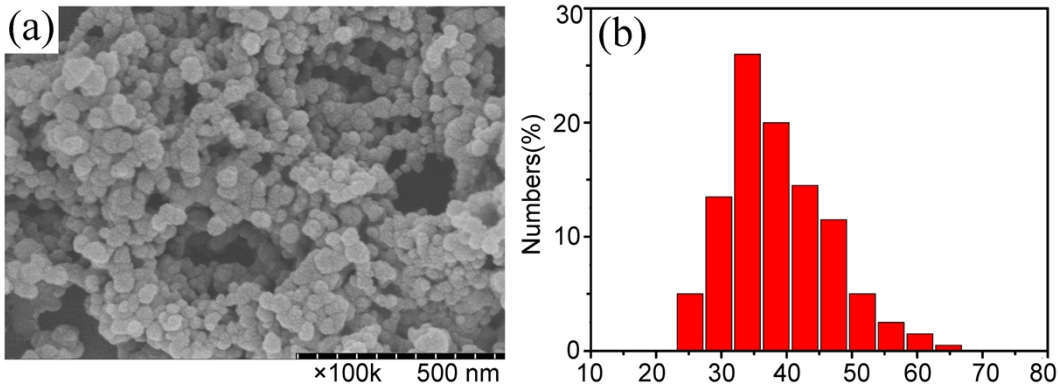

Fig. S7. (a) SEM view of Pd/psf NPs separated from in EtOH/H_2O; (b) Particle size distribution.

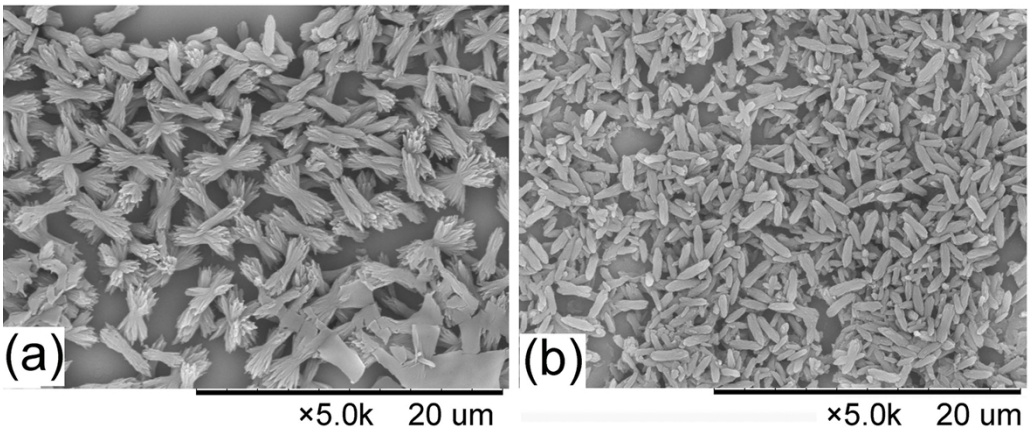

Fig. S8. SEM images of (Pd/psf) NPs separated from EtOH/H_2O at 40°C for 1.0h. (a) for $PdCl_2$ and psf 1.0 mmol/L; (b) for $PdCl_2$ and psf 2.5 mmol/L.

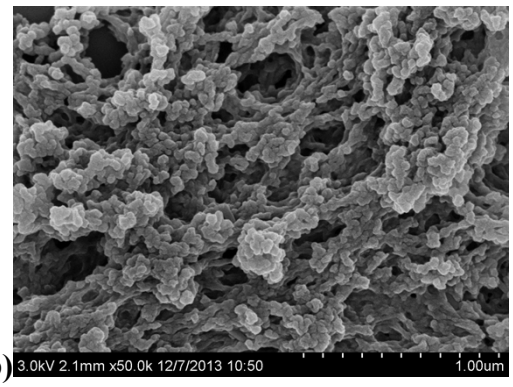

a) **b)**

Fig. S9. SEM image of (Pd/psf) NPs. (a) separated from DMF/H_2O at 90 °C for 10h; (b) separated from CH_2Cl_2/H_2O at 90 °C for 10h.

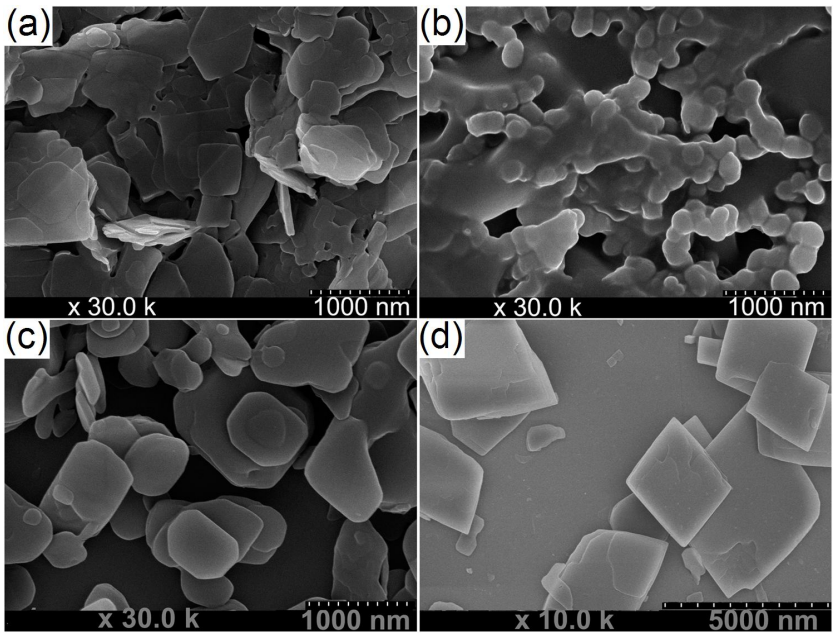

Fig. S10. SEM images of the Cu-psf sheets or colloids obtained from different condition. (a) The size 400 x 300 nm^2 form H_2O-CH_2Cl_2 at 40 °C for 30min; (b) 200 x

200 nm^2 form H_2O-EtOH at 40 ^oC for 30min; (c) 500 x 400 nm^2 form H_2O-CH_2Cl_2 at 90 ^oC for 10h; (d) 2500 x 2500 nm^2 form H_2O-EtOH at 90 ^oC for 10h.

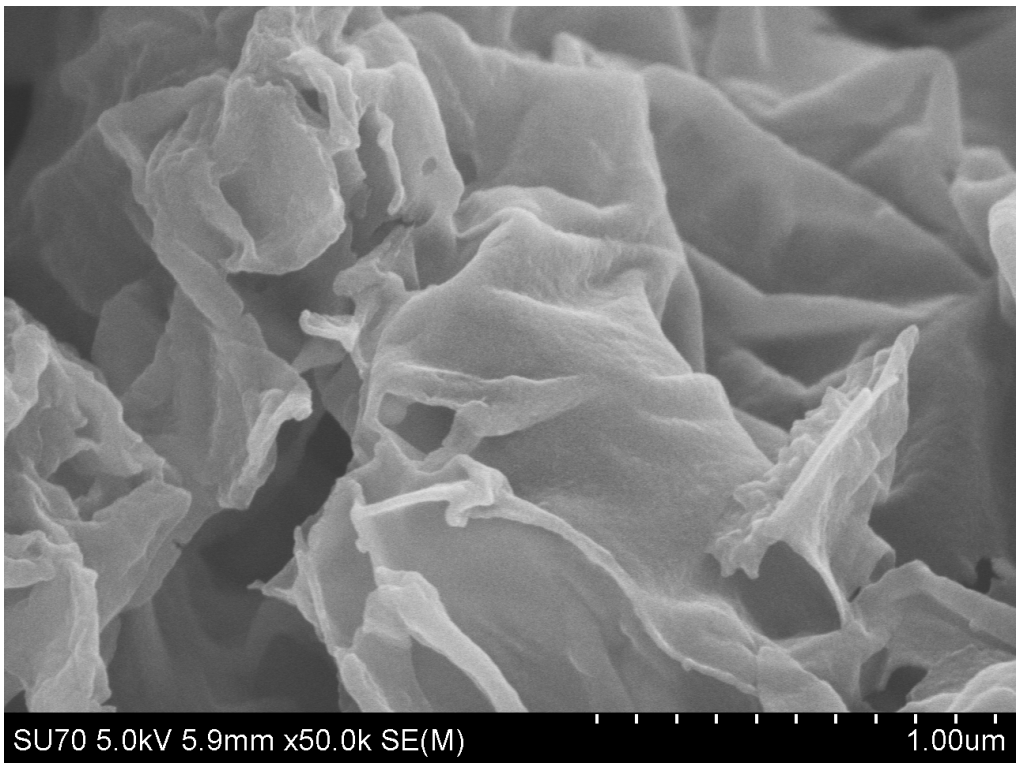

Fig. S11. SEM image of (Cu/Pd/psf) composites.

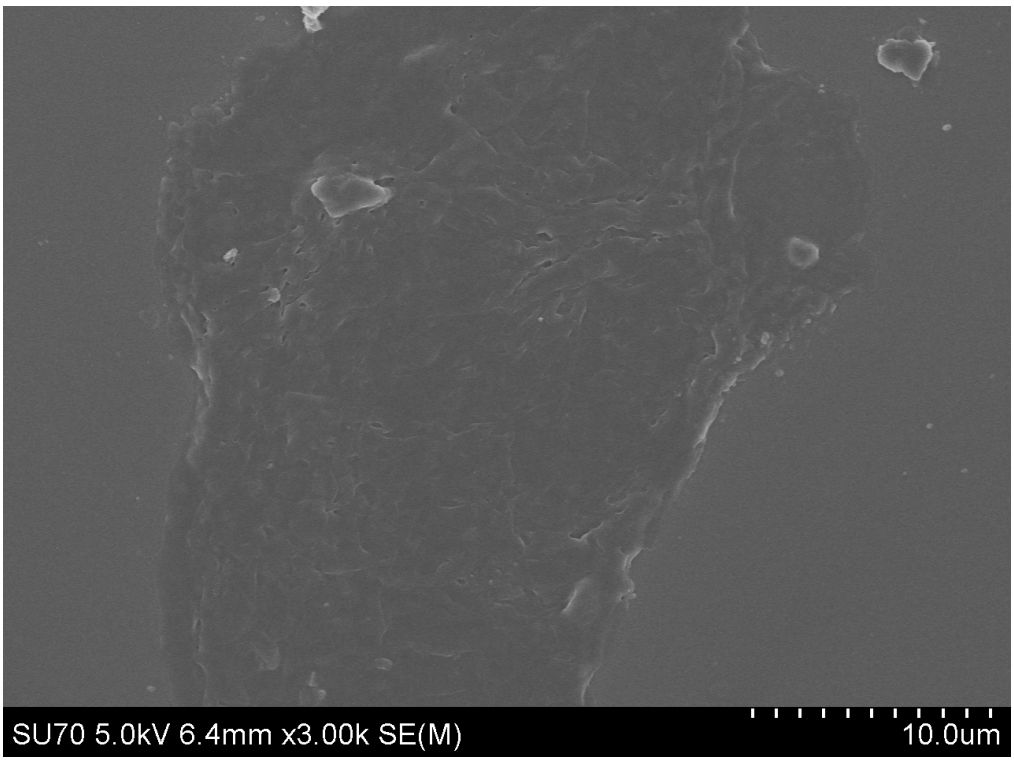

a

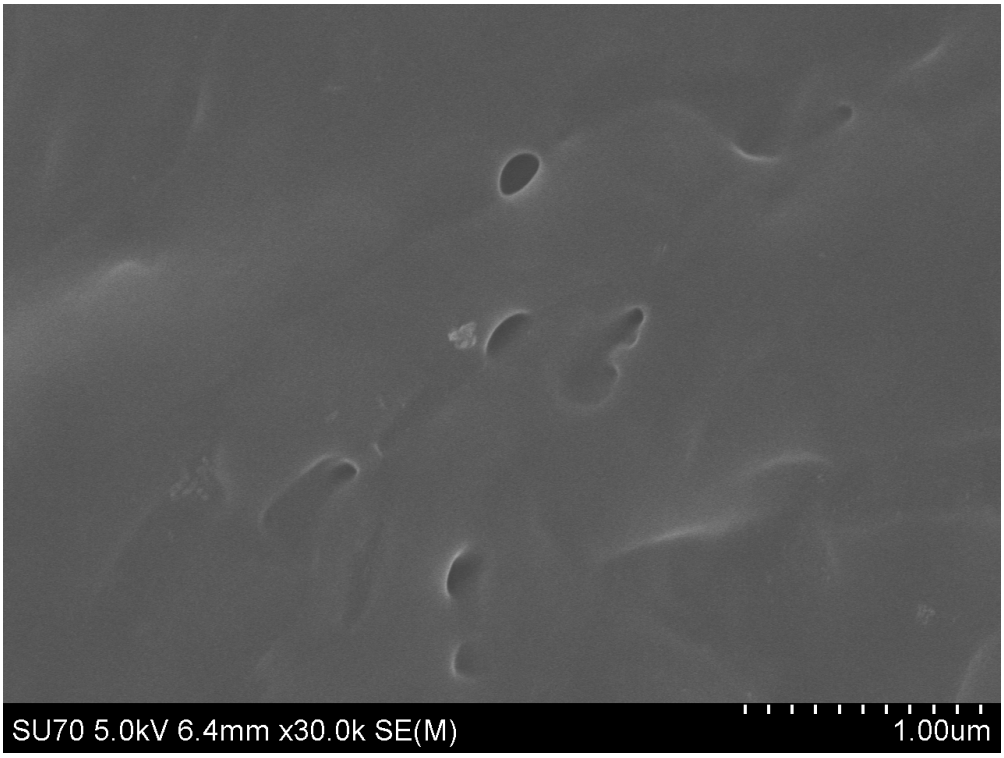

b

Fig. S12. SEM images of the quartz substrate smeared by PEI: a) uneven-distributed, b) well-distributed with PEI.

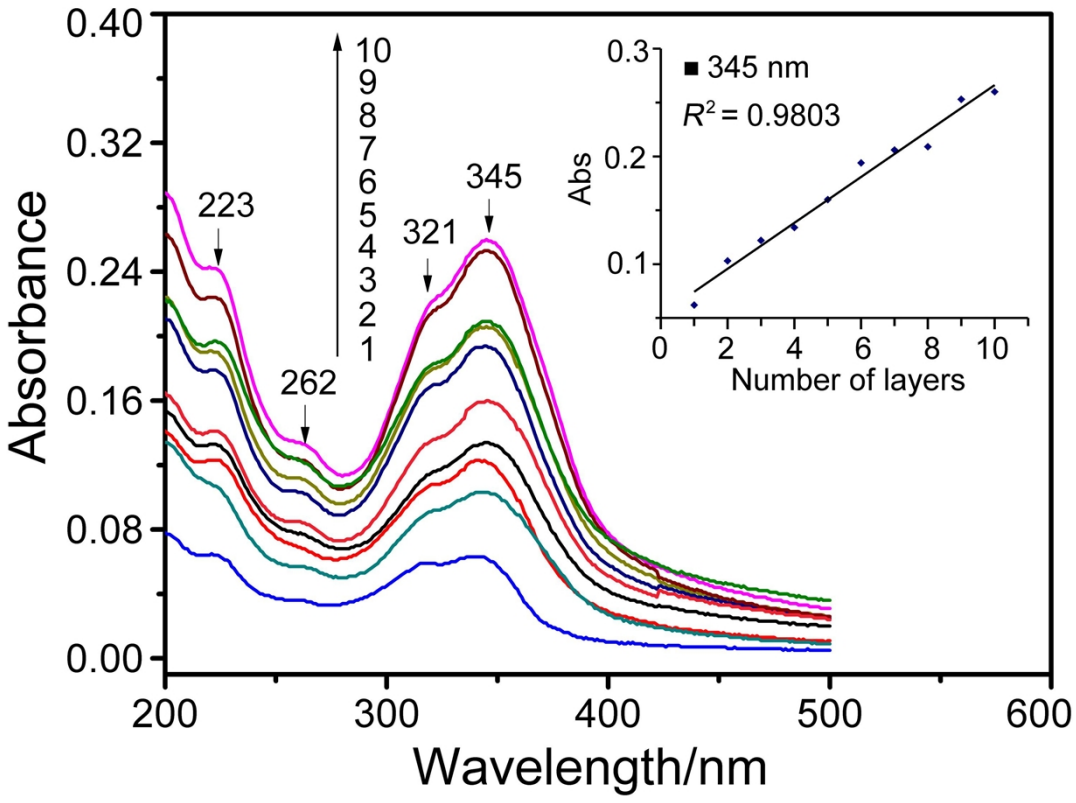

Fig. S13. UV-vis spectra of films PEI-$[Cu(NO_3)_2/psf]_n$ (n = 10).

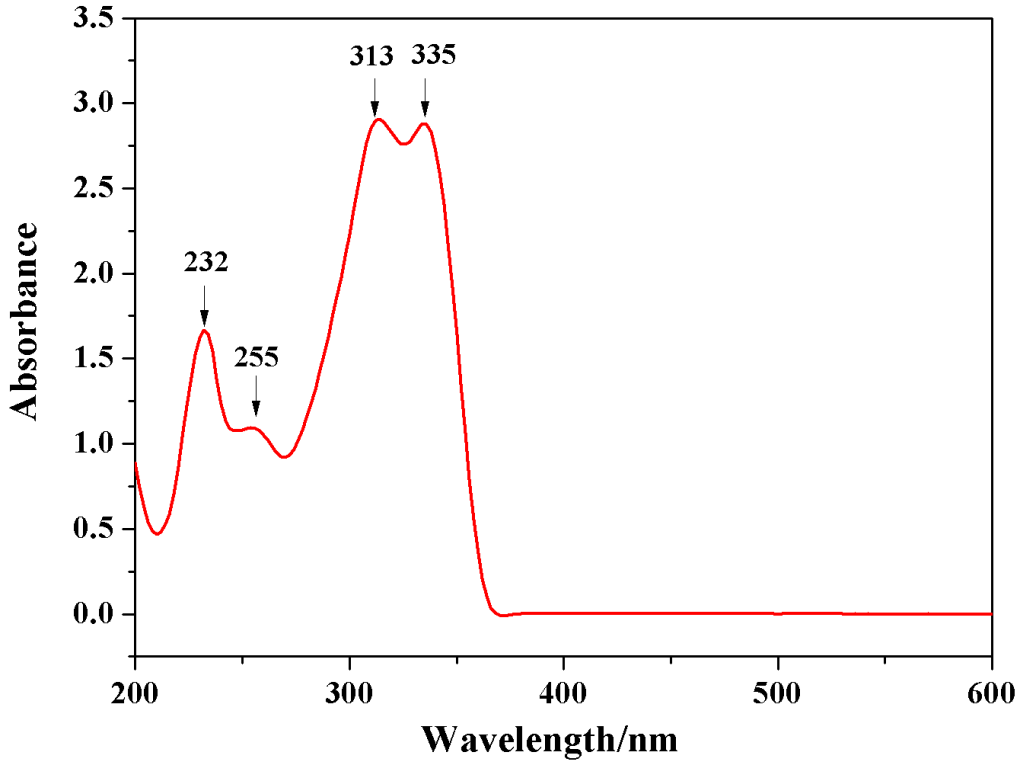

Fig. S14. UV-vis spectra of psf in CH_2Cl_2.

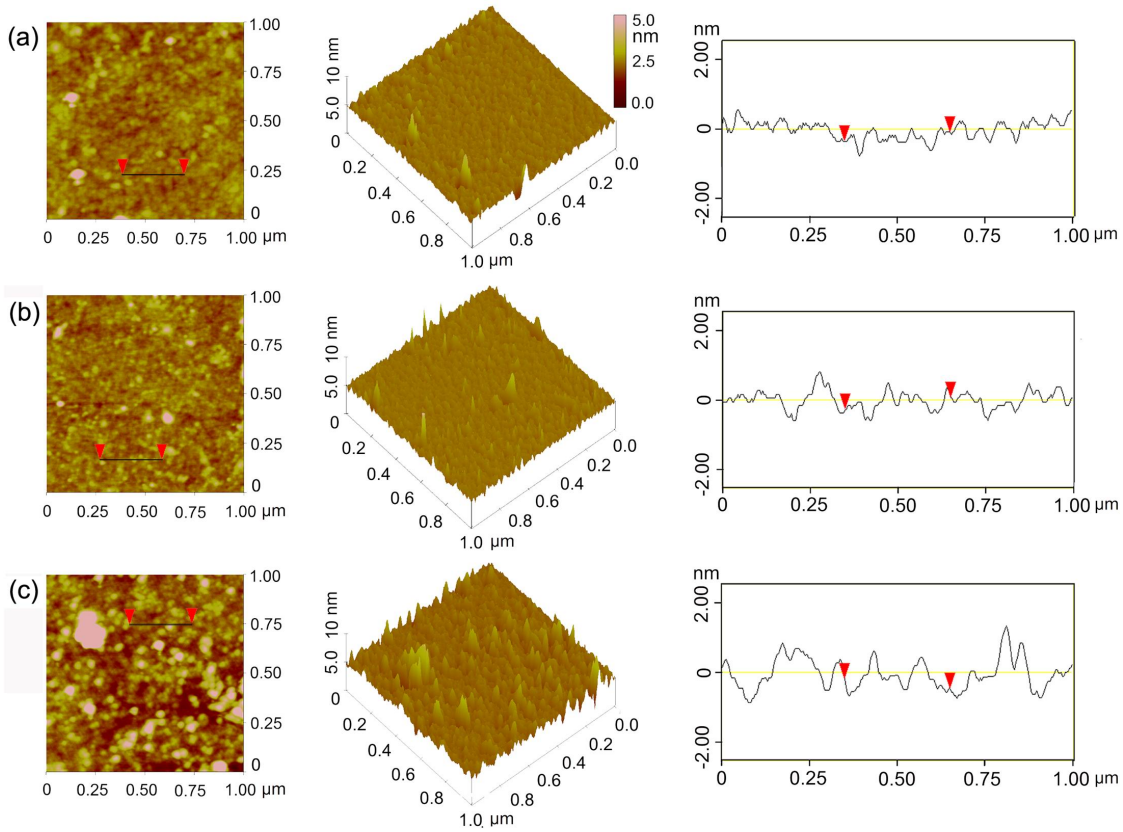

Fig. S15. AFM images of the films. (a) $(Cu^{2+}/psf)_5$ (R_{rms} = 0.430 nm, R_{max} = 6.615 nm). (b) $(Cu^{2+}/psf)_{10}$ (R_{rms} = 1.134 nm, R_{max} = 16.325 nm). (c) $(Cu^{2+}/psf)_{15}$ (R_{rms} = 1.293 nm, R_{max} = 25.461 nm).

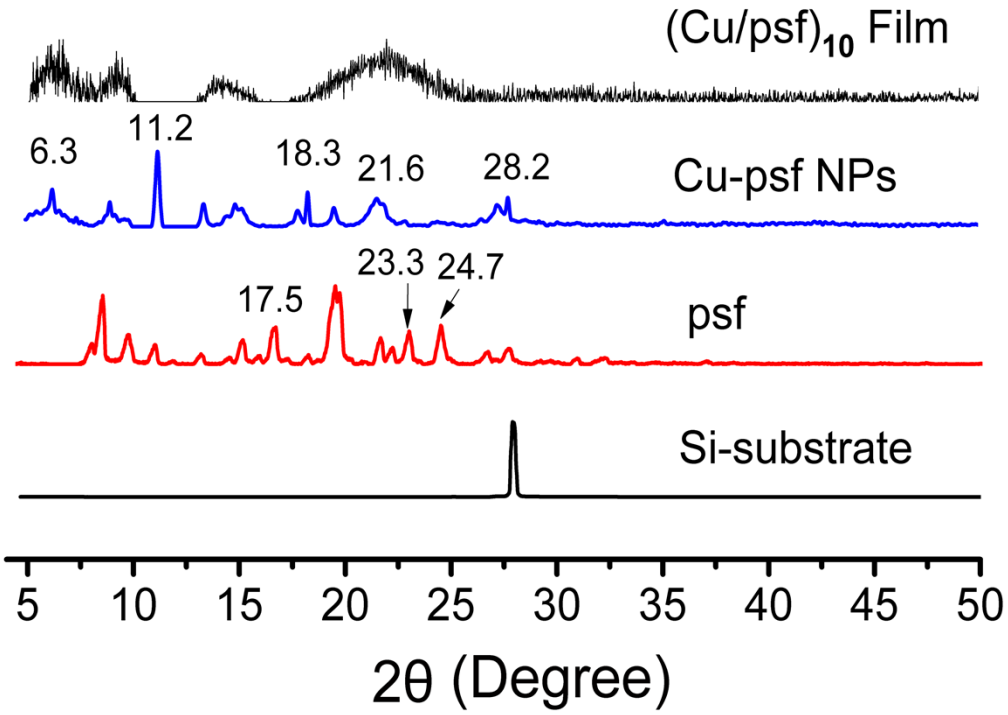

Fig. S16. PXRD patterns. CuO peaks: 16.6, 23.8.; $Cu(OH)_2$ peak: 6.9

Table S3. Screening of Cu-catalysts for the coupling reactions of aryl iodides with aryl boronic acids.

Entry	Catalyst	T/ºC	Time/h	Yield/%
1	Cu powder	90	10	Trace
2	Cu powder + psf	90	10	47
3	CuI	90	10	Trace
4	CuI + psf	90	10	99
5	$Cu(NO_3)_2$	90	10	0
6	$Cu(NO_3)_2$/psf sheets	90	10	95
7	$CuSO_4$	90	10	0
8	$CuSO_4$/psf	90	10	34
9	$CuCl_2$	90	10	0
10	$CuCl_2$/psf	90	10	26

Typical procedure: 1.0 mmol of aryl iodobe, 1.2 mmol of aryl boronic acid, 3.0 mmol of K_2CO_3, 0.03 mmol of catalysts (3.0% metal or metal-ligand nanoparticles relative to aryl iodobe), 4.0 mL of EtOH and 3.0 mL of H_2O.

Table S4. Effect of nanoparticulate dimensional sizes of Cu-psf combination on the yields in the coupling reactions.

Entry	Catalyst	Size	T/ºC	Time/h	Yield/%
1	Cu-psf sheets	200 x 200 nm^2 (Fig. 5b)	90	10	83±3
2	Cu-psf sheets	400 x 300 nm^2 (Fig. 5a)	90	10	71±3
3	Cu-psf sheets	500 x 400 nm^2 (Fig. 5c)	90	10	65±3
4	Cu-psf sheets	2500 x 2500 nm^2 (Fig. 5d)	90	10	58±5

Aryl iodide (1.0 mmol), arylboronic acid (1.2 mmol), K_2CO_3 (3.0 mmol) in H_2O / EtOH at 90°C for 10h. Catalyst-loading 3.0%.

Table S5. Effect of amount of catalysts on the coupling reaction of aryl iodides with aryl boronic acids using [$Cu(NO_3)_2$/psf] nanoparticulates as catalysts.

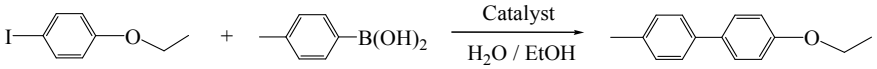

Entry	Cu-loading (mmol %)	T (°C)	Time (h)	Yield (%)
1	2.9	90	10	95
2	2.9×10^{-1}	90	10	90
3	2.9×10^{-2}	90	10	89
4	2.9×10^{-3}	90	10	<5
5	2.9×10^{-4}	90	10	<3

General procedure: Aryl iodide (1.0 mmol), arylboronic acid (1.2 mmol), K_2CO_3 (3.0 mmol) in H_2O / EtOH at 90°C for 10h. Cu(II) : psf = 1:1 (mol/mol).

Table S6. Effect of the co-catalysts and temperatures on the coupling reactions of aryl iodides with aryl boronic acids under ambient atmosphere for 10 hours.

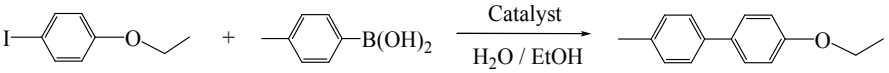

Entry	Catalyst	T / °C	Yield (%)
1	$Cu(NO_3)_2/PPh_3$ NPs	90	0
2	$Cu(NO_3)_2$/bpy NPs	50/70 /90	0 / 4 / 31
3	$Cu(NO_3)_2$/psf sheets	50/70 /90	5 / 87 / 95
4	$(Cu(NO_3)_2/psf)_{10}$ film	50/70 /90	12 / 90 / 99

Procedure: aryl iodide (1.0 mmol), arylboronic acid (1.2 mmol), K_2CO_3 (3.0 mmol), in H_2O / EtOH (4:3, V/V). bpy = 4,4'-bipyridine. Catalyst-loading 3.0% for $Cu(NO_3)_2/PPh_3$ NPs, $Cu(NO_3)_2$/bpy NPs and $Cu(NO_3)_2$/psf sheets; 1.4 x 10^{-5} mol% $(Cu(NO_3)_2/psf)_{10}$ film.

IR and NMR of the coupling products

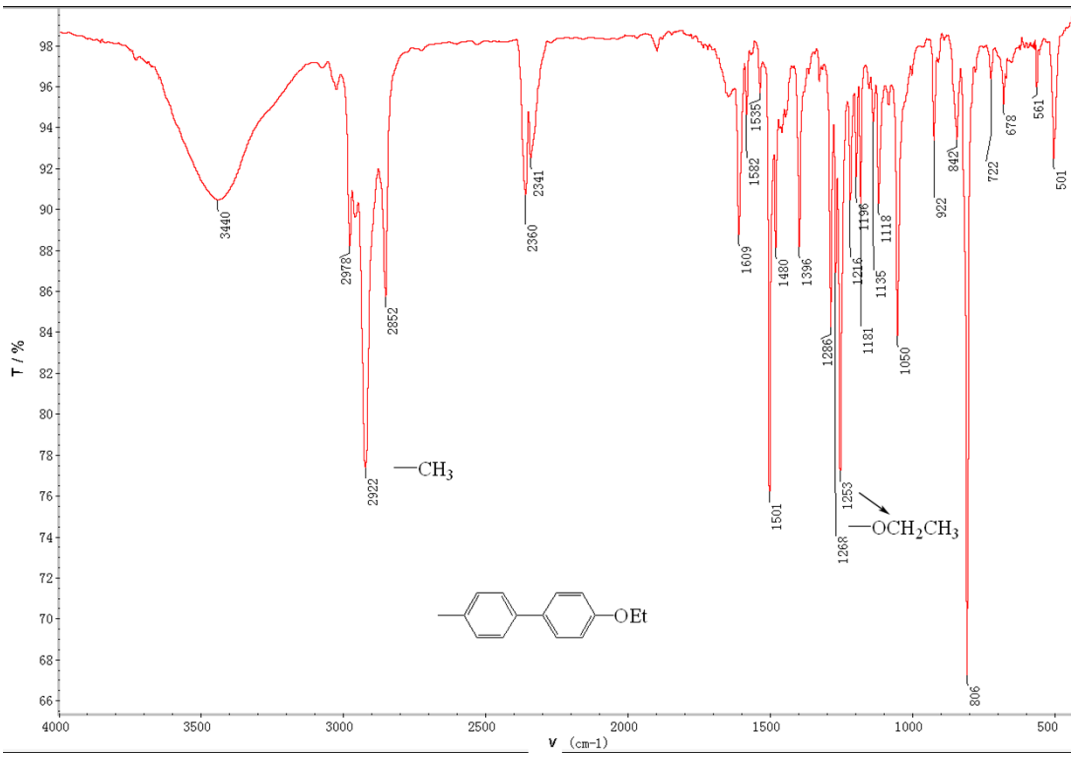

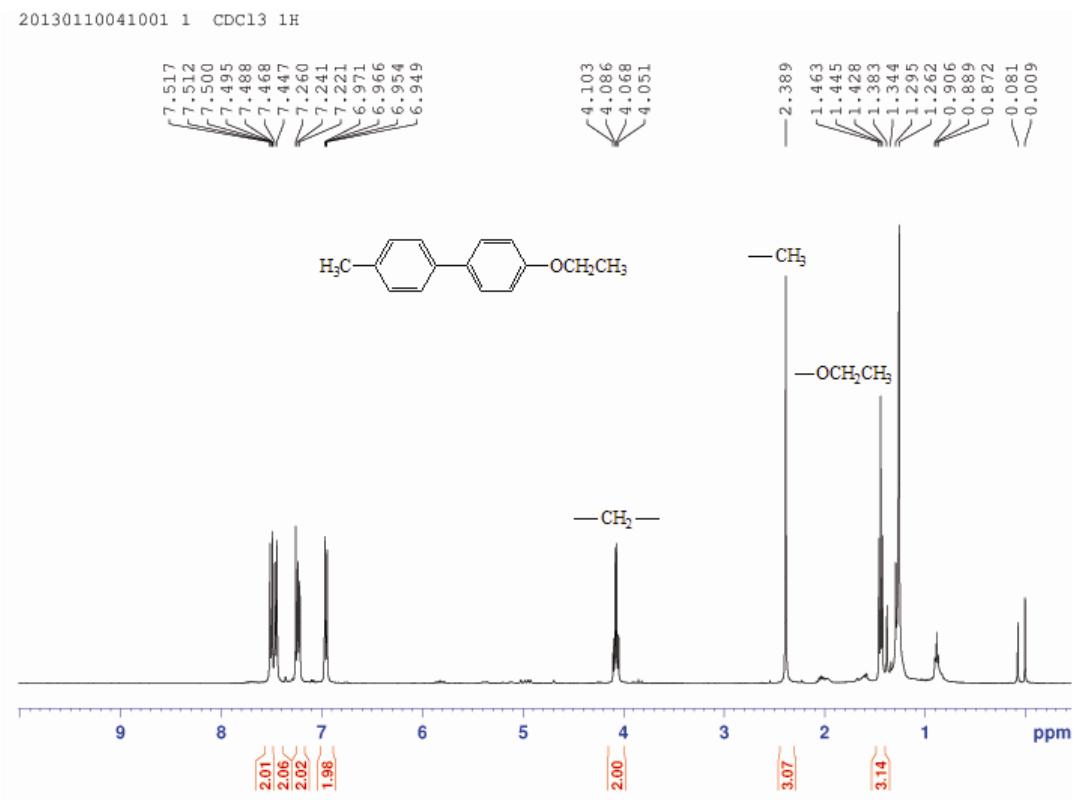

^{1}H NMR ($CDCl_3$, 400 MHz): δ = 7.517-7.512 (d, 2H, -C_6H_4), 7.500-7.495 (d, 2H, -C_6H_4), 7.260-7.241 (d, 2H, -C_6H_4), 6.966-6.954 (d, 2H, -C_6H_4), 4.103-4.051 (q, 2H, -CH_2), 2.389 (s, 3H, -CH_3), 1.463-1.428 (t, 3H, -CH_3) ppm.

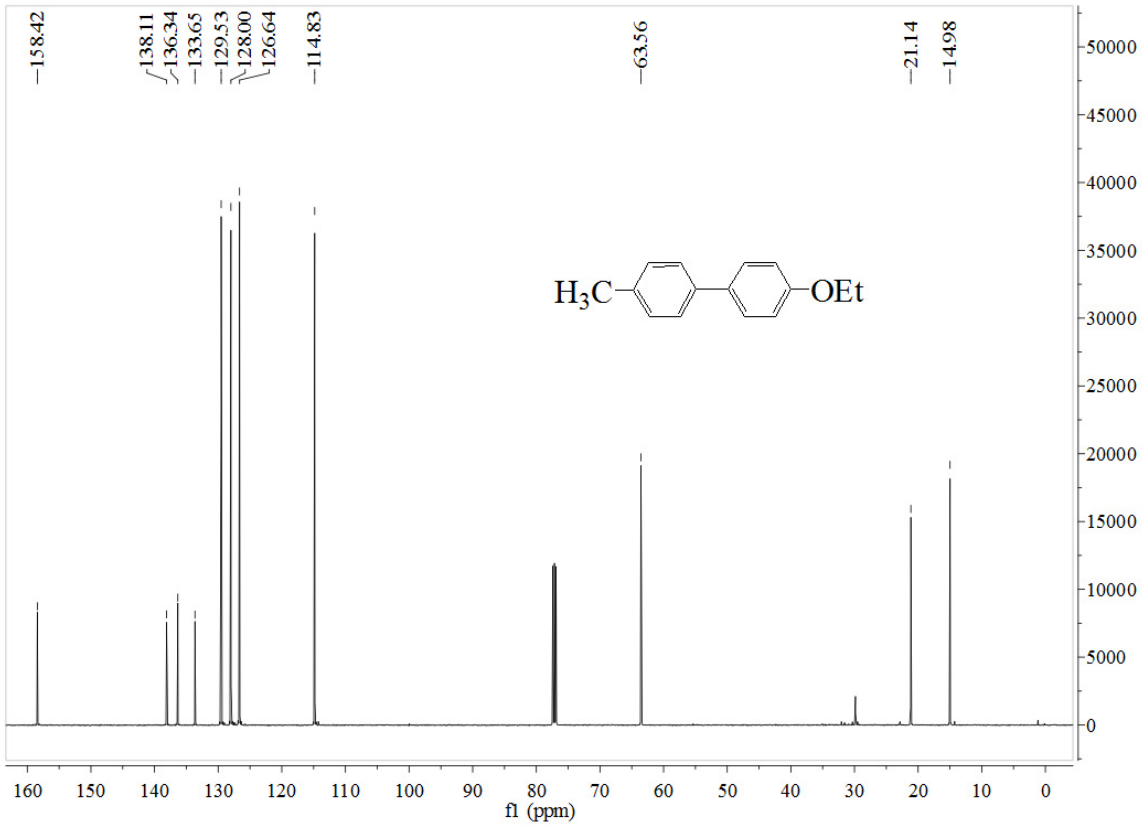

^{13}C NMR ($CDCl_3$, 125 MHz): δ = 158.42 (C-O), 138.11 (C), 136.34 (C), 133.65 (CH), 129.53 (CH), 128.00 (C), 126.64 (CH), 114.83 (CH), 63.56 (CH_2), 21.14 (CH_3), 14.98 (CH_3) ppm.

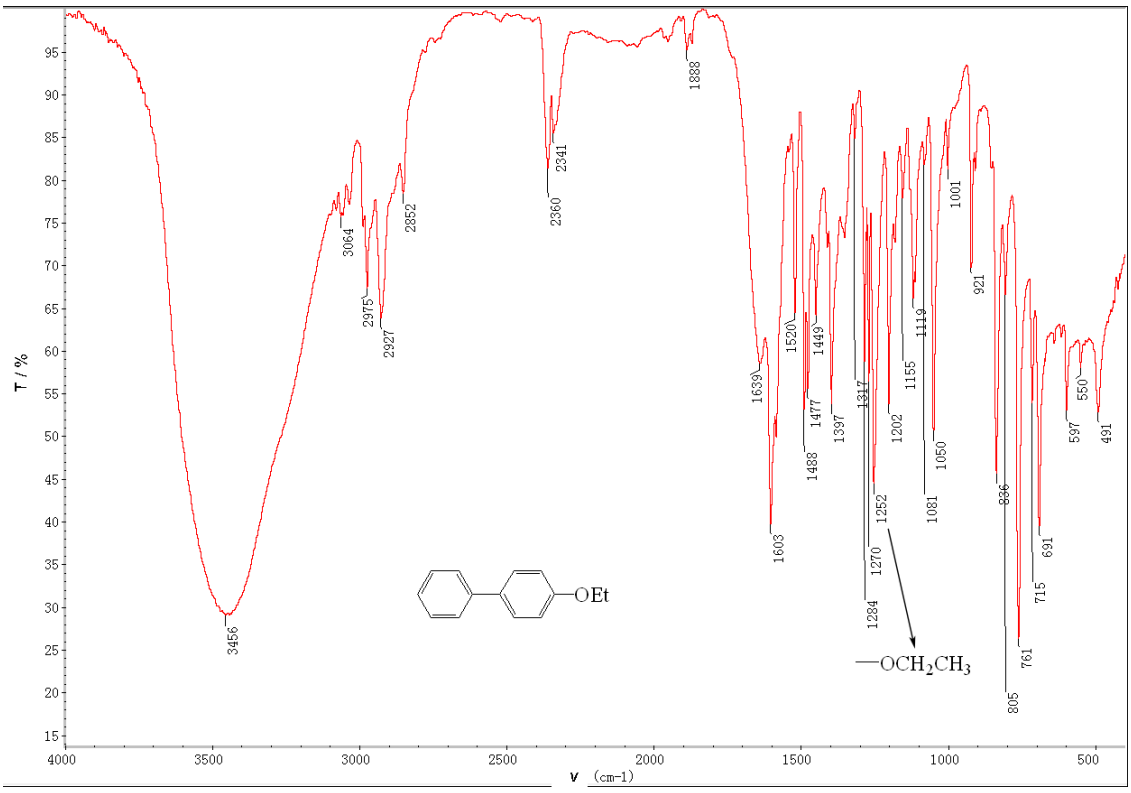

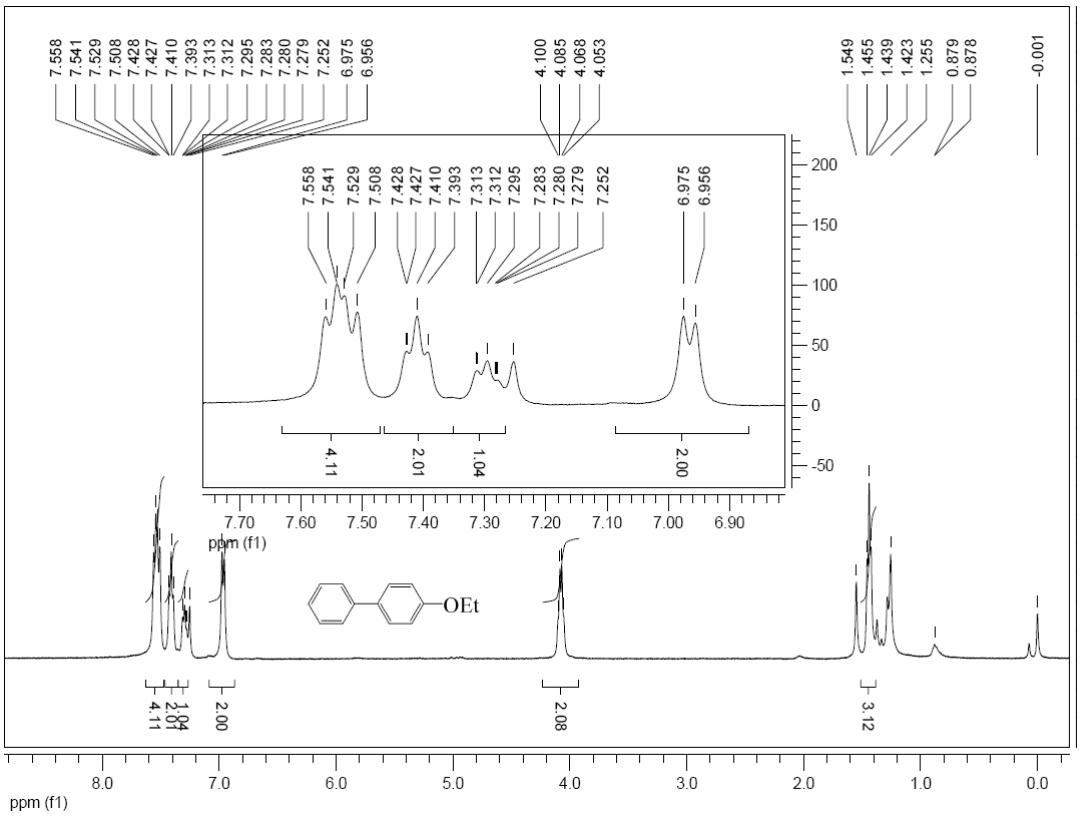

^{1}H NMR ($CDCl_3$, 400 MHz): δ = 7.558-7.508 (m, 4H, -C_6H_5, -C_6H_4) , 7.427-7.393 (t, 2H, -C_6H_5) , 7.312-7.283 (t, 1H, -C_6H_5) , 6.975-6.956 (d, 2H, -C_6H_2), 4.100-4.053 (q, 2H, -CH_2), 1.455-1.423 (t, 3H, -CH_3) ppm.

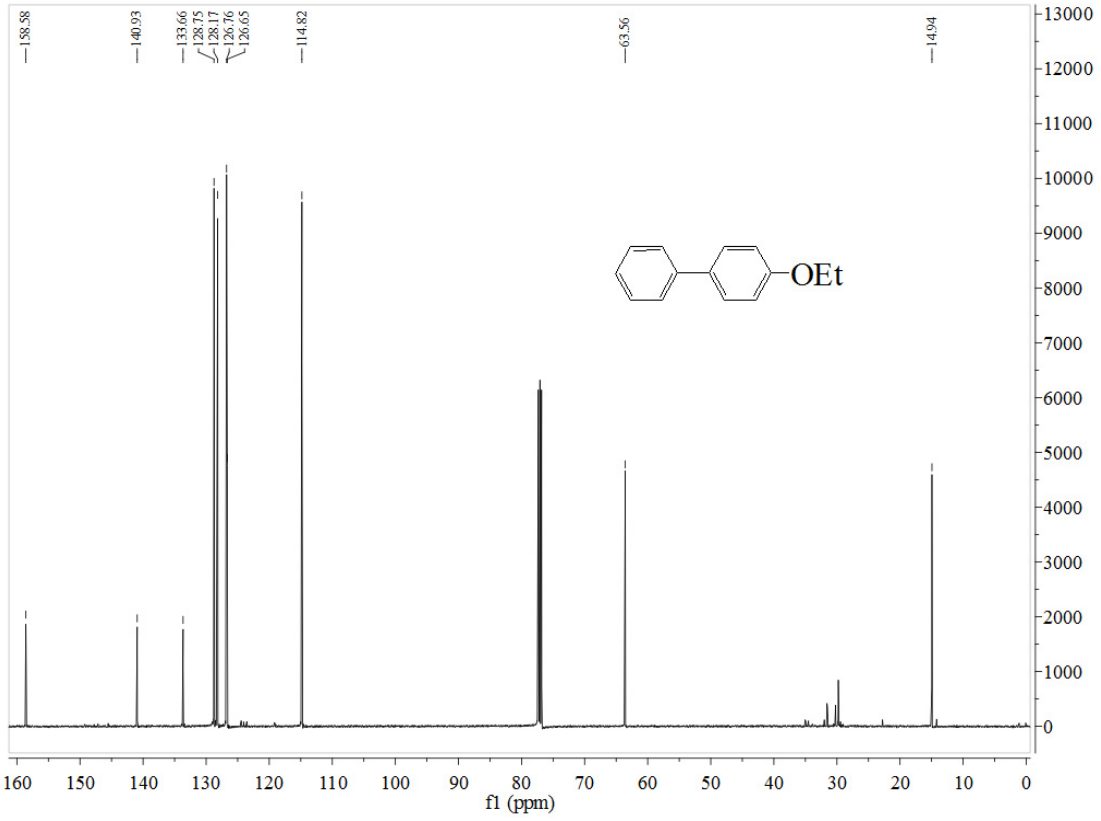

^{13}C NMR ($CDCl_3$, 125 MHz): δ = 158.58 (C-O), 140.93 (C), 133.66 (CH), 128.75 (CH), 128.17 (C), 126.76 (CH), 126.65 (CH), 114.82 (CH), 63.56 (CH_2), 14.94 (CH_3) ppm.

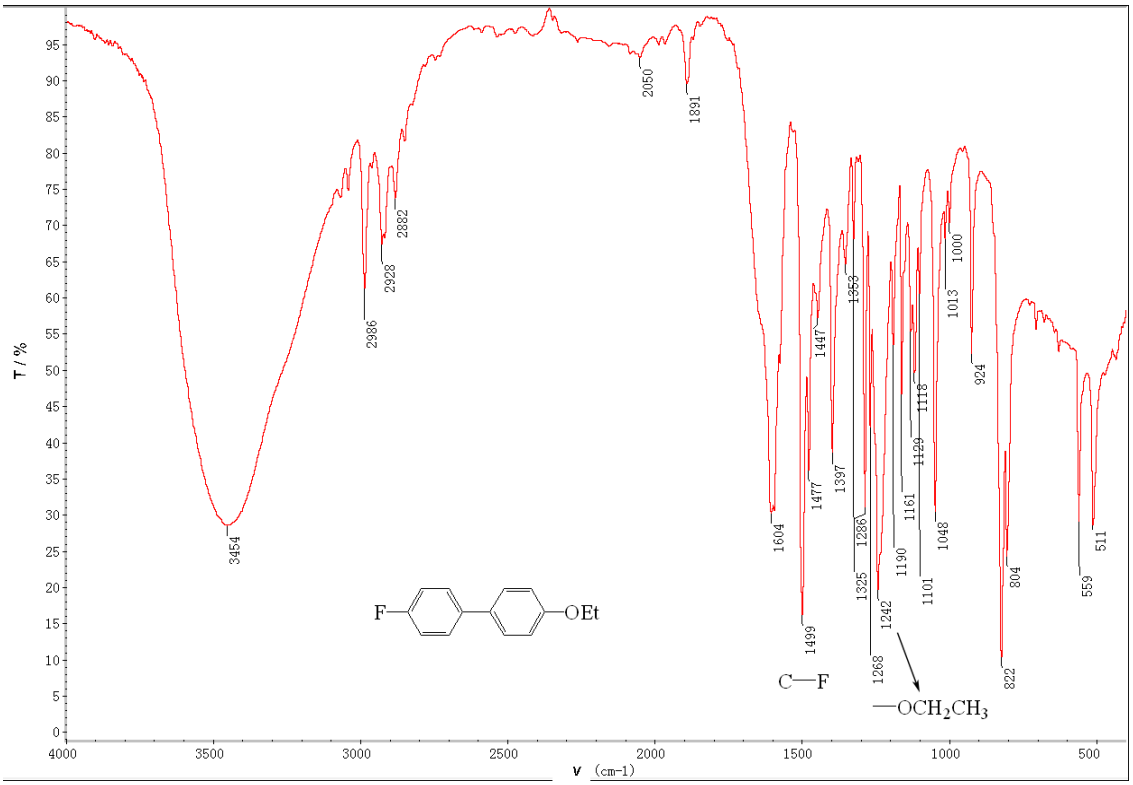

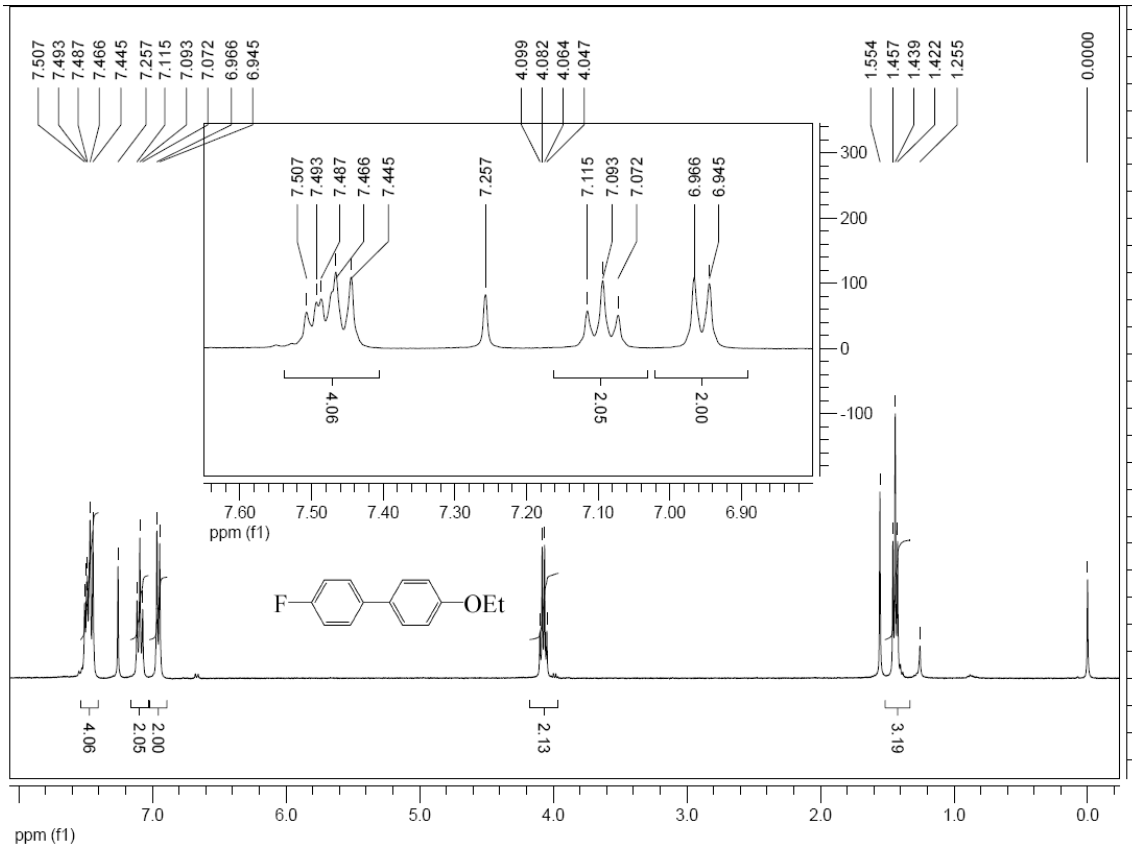

^{1}H NMR ($CDCl_3$, 400 MHz): δ = 7.507-7.445 (m, 4H, -C_6H_4, -C_6H_4F), 7.115-7.072 (t, 2H, -C_6H_4F), 6.966-6.945 (d, 2H, -C_6H_4), 4.099 ~ 4.047 (q, 2H, -CH_2), 1.457-1.422 (t, 3H, -CH_3) ppm.

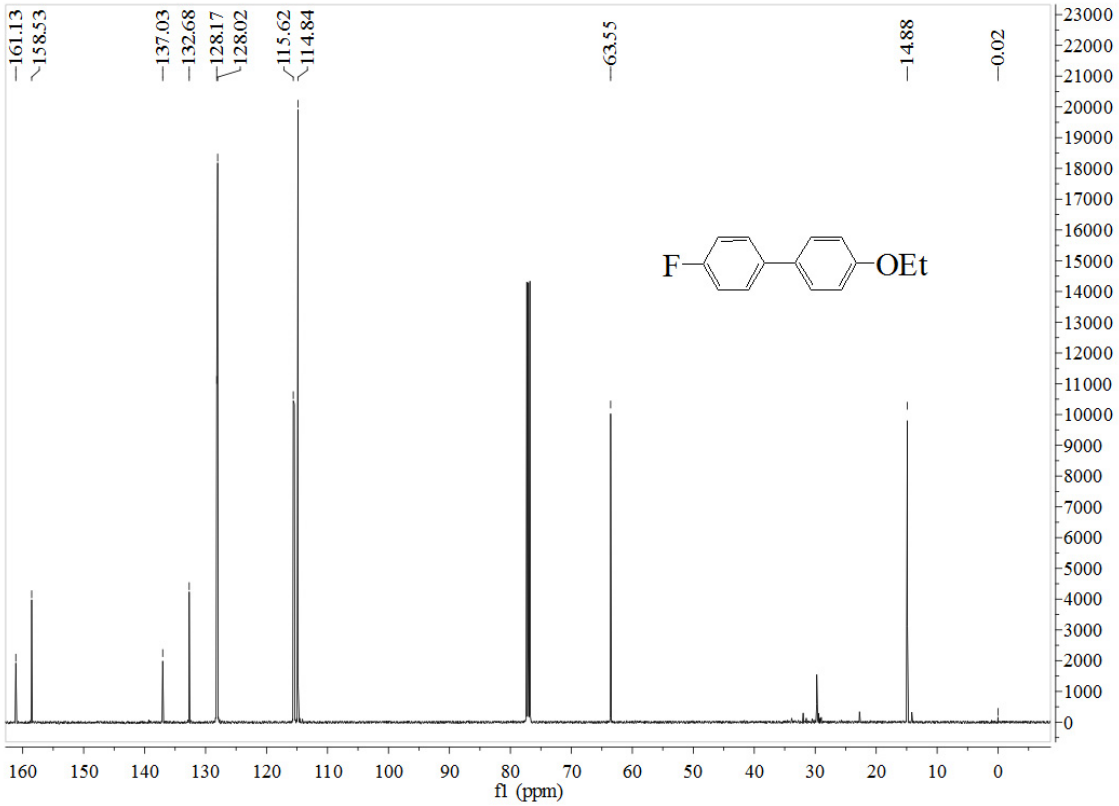

^{13}C NMR ($CDCl_3$, 125 MHz): δ = 161.13 (C-F), 158.53 (C-O), 137.03 (C), 132.68 (CH), 128.17 (CH), 128.02 (C), 115.62 (CH), 114.84 (CH), 63.55 (CH_2), 14.88 (CH_3) ppm.

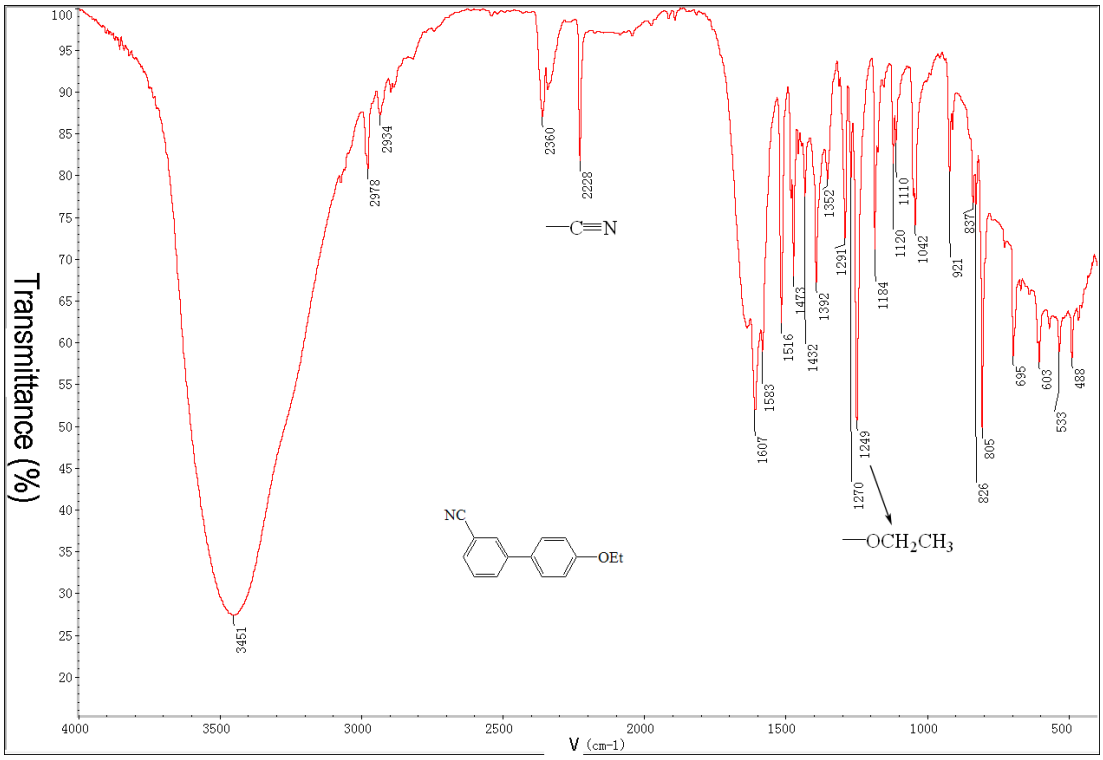

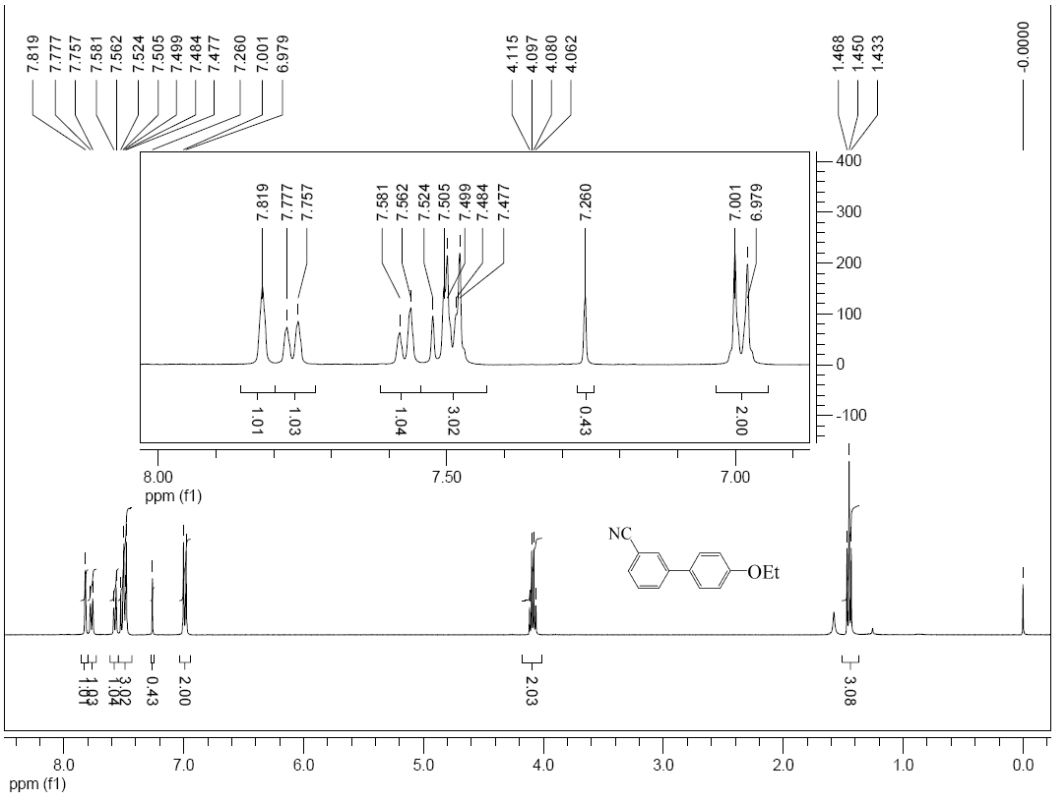

^{1}H NMR ($CDCl_3$, 400 MHz): δ = 7.819 (s, 1H, -C_6H_4CN), 7.777-7.757 (d, 1H, -C_6H_4CN), 7.581-7.477 (m, 4H, -C_6H_4), 7.001-6.979 (d, 2H, -C_6H_4), 4.115-4.062 (q, 2H, -CH_2), 1.46-1.433 (t, 3H, -CH_3) ppm.

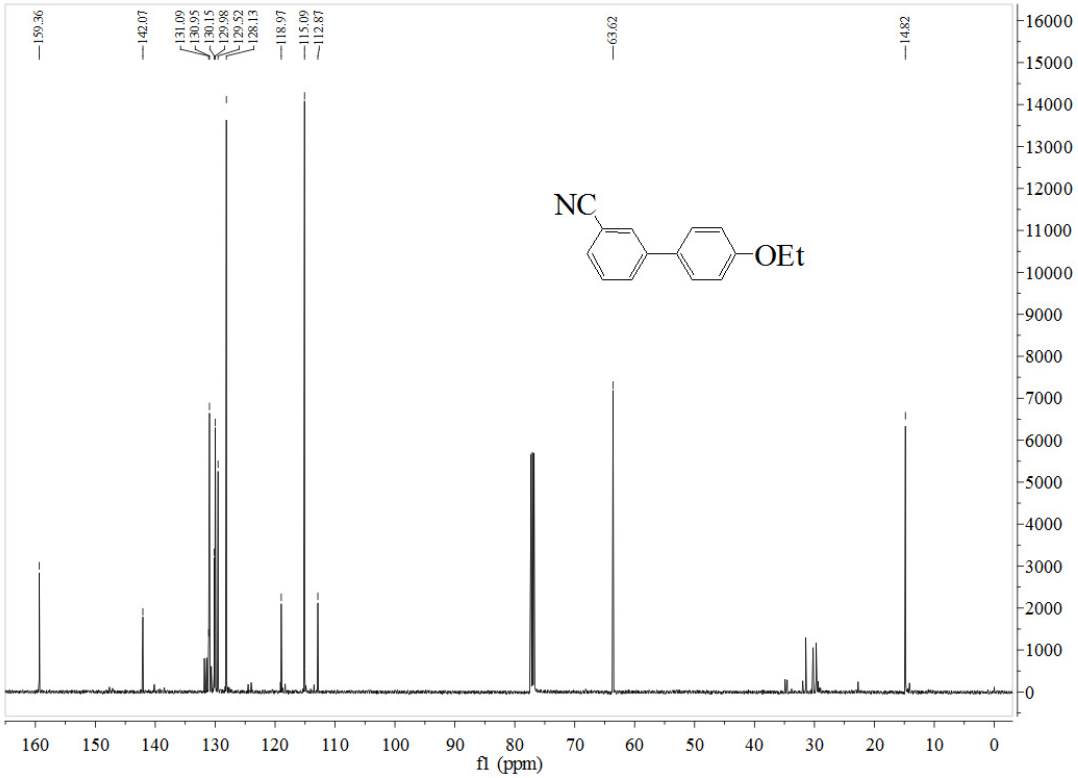

^{13}C NMR ($CDCl_3$, 125 MHz): δ = 159.36 (C-O), 142.07 (C), 131.09 (CH), 130.95 (CH), 130.15 (CH), 129.98 (CH), 129.52 (CH), 128.13 (C), 118.97 (CN), 115.09 (CH), 112.87 (C), 63.57 (CH_2), 14.78 (CH_3) ppm.

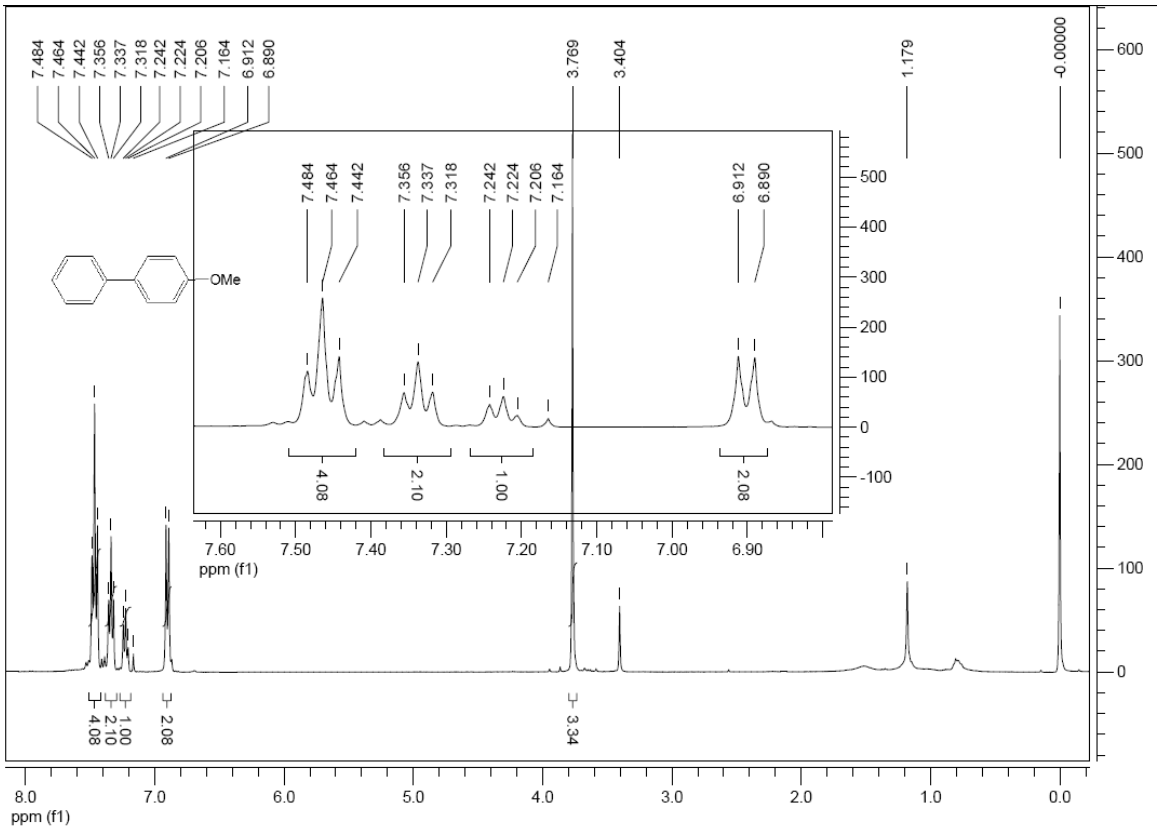

^{1}H NMR ($CDCl_3$, 400 MHz): δ = 7.484-7.442 (m, 4H, -C_6H_4, -C_6H_5), 7.356-7.318 (t, 2H, -C_6H_5), 7.242-7.206 (t, 1H, -C_6H_5), 6.912-6.890 (d, 2H, -C_6H_4), 3.769 (s, 3H, -CH_3) ppm.

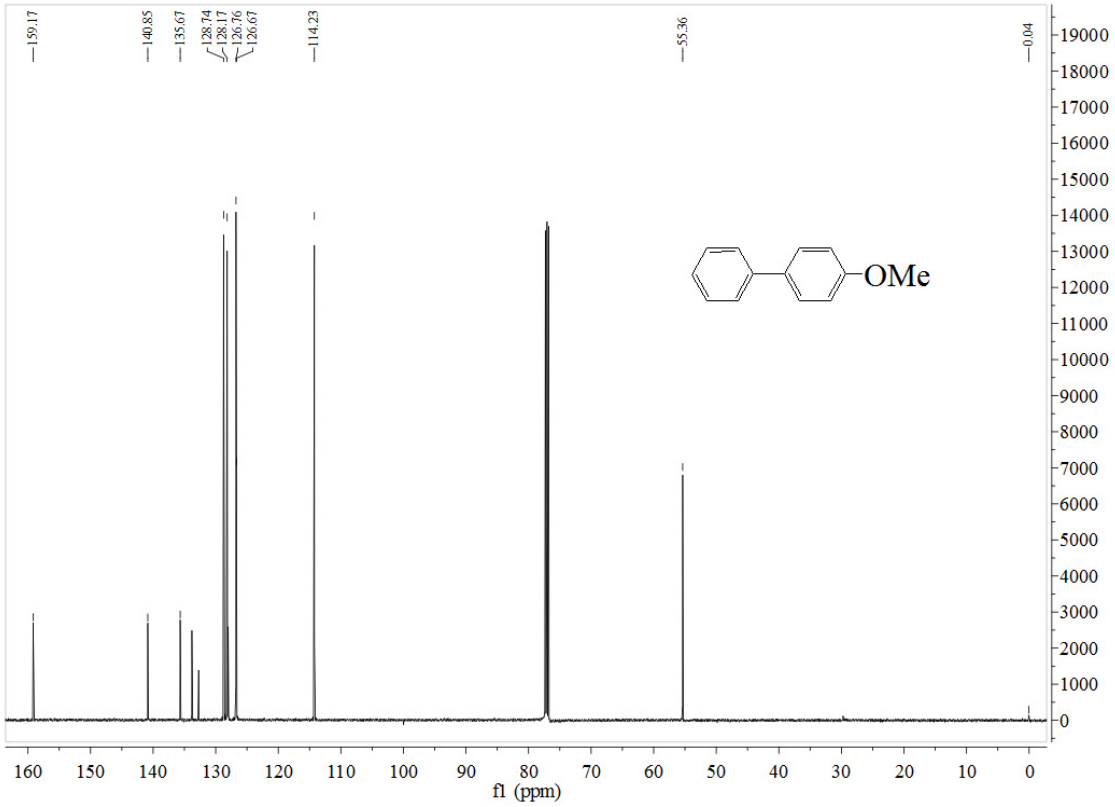

^{13}C NMR ($CDCl_3$, 125 MHz): δ = 159.17 (C-O), 140.85 (C), 135.67 (CH), 128.74 (CH), 128.17 (C), 126.76 (CH), 126.67 (CH), 114.23 (CH), 55.36 (CH_3) ppm.

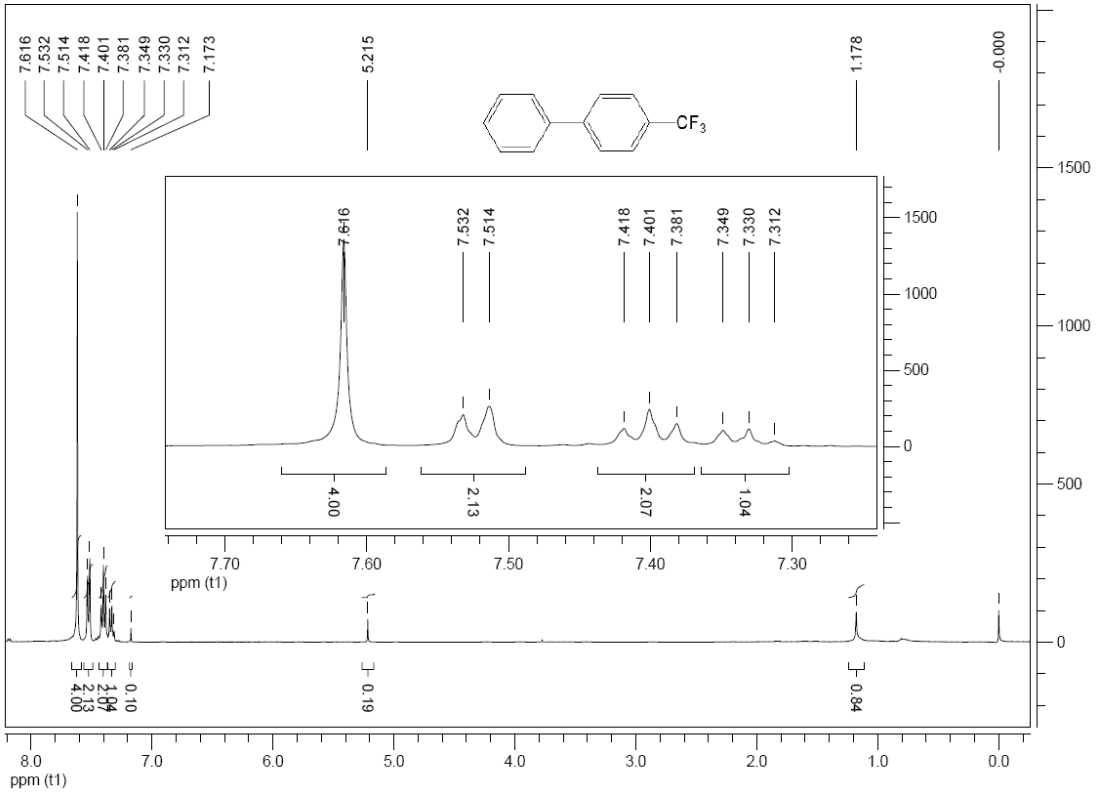

^{1}H NMR ($CDCl_3$, 400 MHz): δ = 7.616 (s, 4H, -C_6H_4, -C_6H_5), 7.532-7.514 (d, 2H, -C_6H_4), 7.418-7.381 (t, 2H, -C_6H_5), 7.349-7.312 (t, 1H, -C_6H_5) ppm.

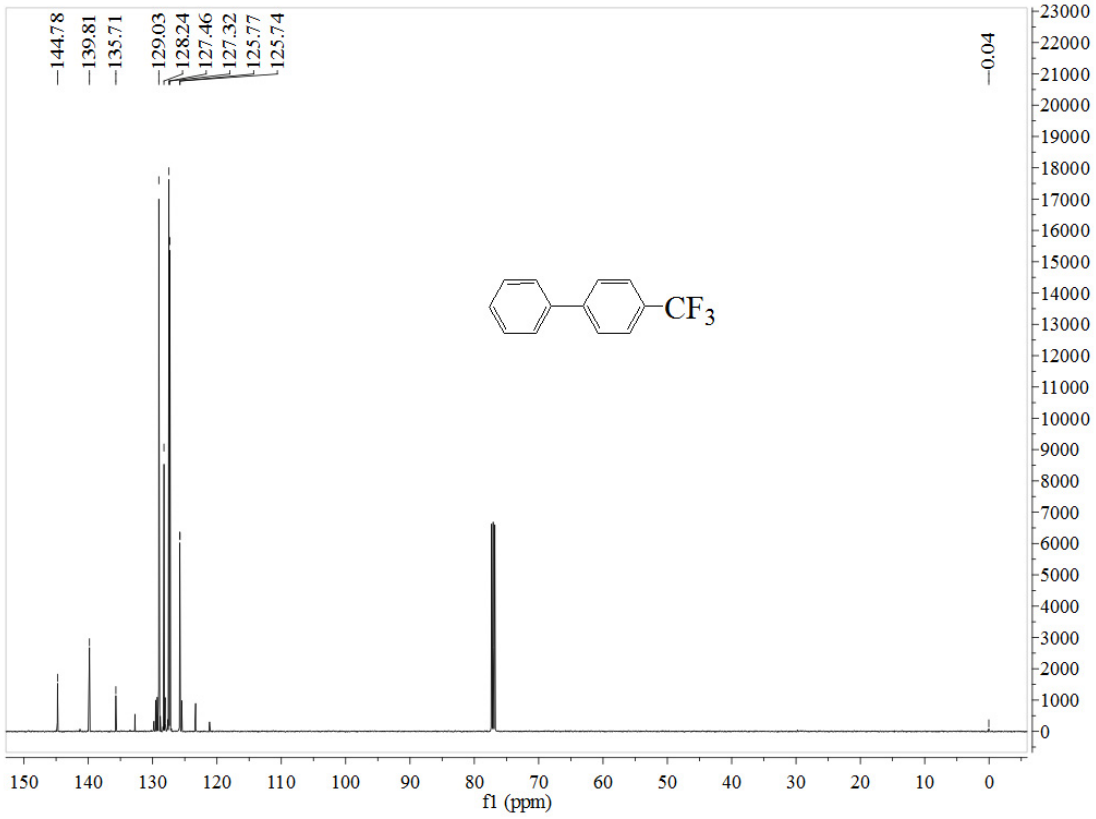

^{13}C NMR ($CDCl_3$, 125 MHz): δ = 144.78 (C), 139.81 (C), 135.71 (C), 129.03 (CH), 128.24 (CH), 127.46 (CH), 127.32 (CH), 125.77 (CH), 125.74 (CF_3) ppm.

GC-MS of the coupling products

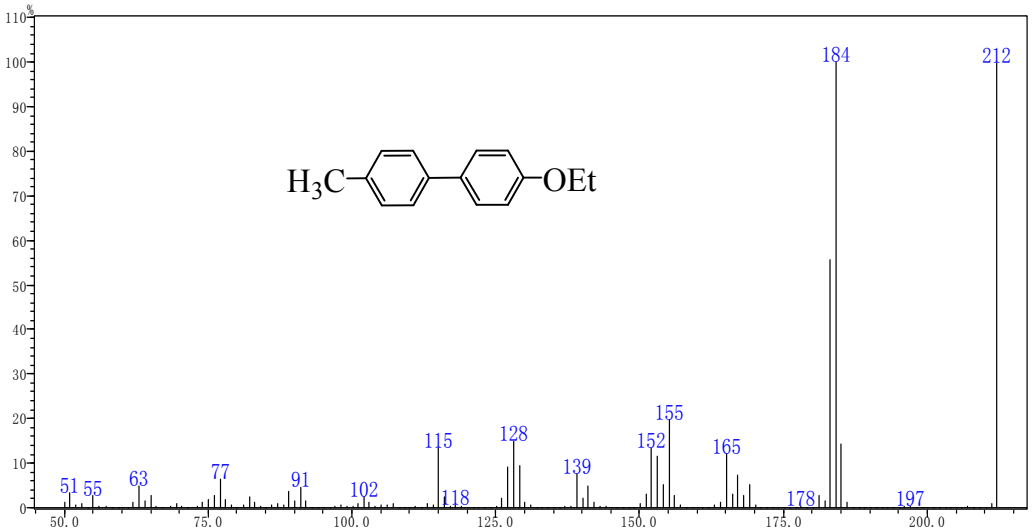

MS (ESI): m/z calcd for M = $C_{15}H_{16}O$: 212.29; found 212 (M), 184 (M + H^+ - Et^-).

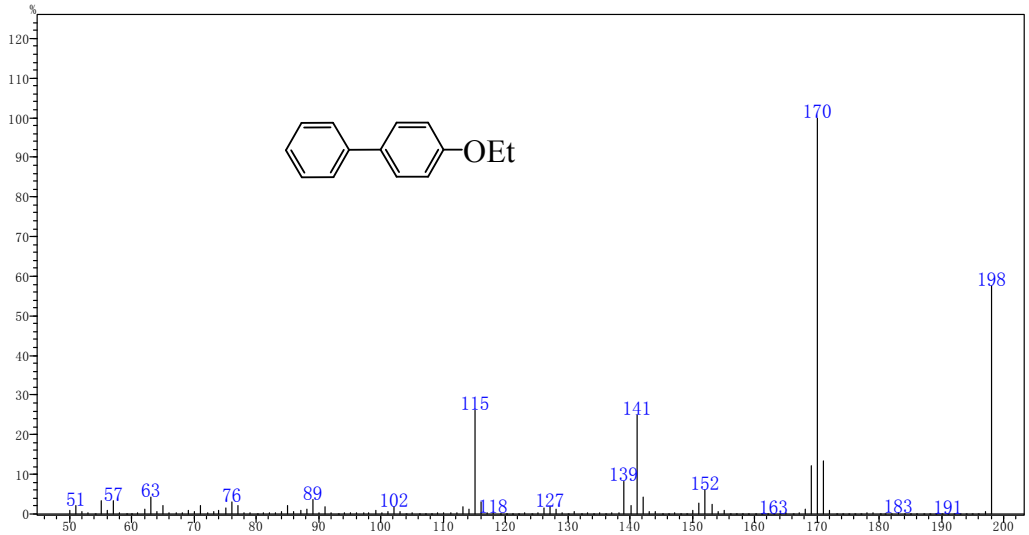

MS (ESI): m/z calcd for M = $C_{14}H_{14}O$: 198.26; found 198 (M), 170 (M + H^+ - Et^-).

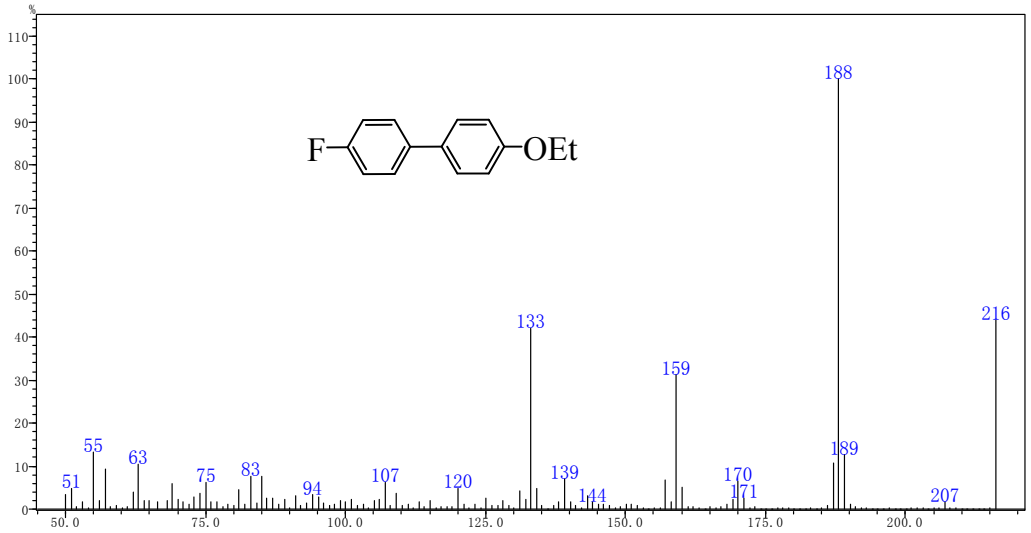

MS (ESI): m/z calcd for M = $C_{14}H_{13}OF$: 216.26; found 216 (M), 188 (M + H^+ - Et^-).

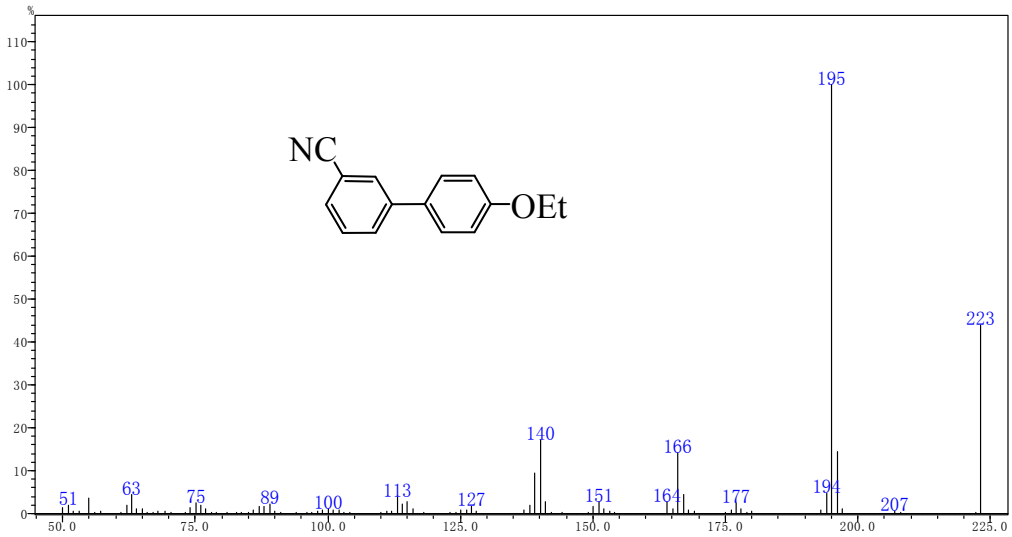

MS (ESI): m/z calcd for M = $C_{15}H_{13}ON$: 223.27; found 223 (M), 195 (M + H^+ - Et^-).

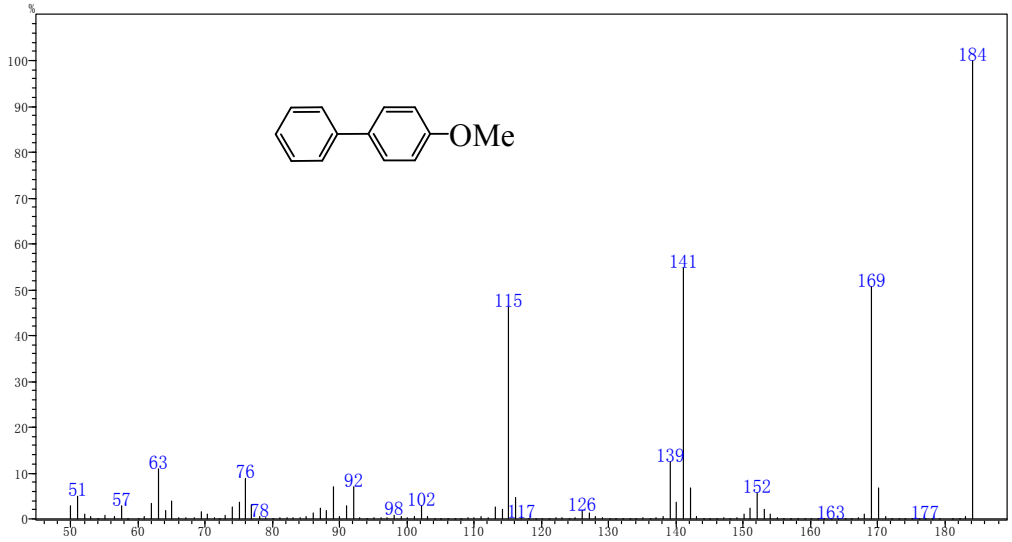

MS (ESI): m/z calcd for M = $C_{13}H_{12}O$: 184.24; found 184 (M), 169 (M – Me^-).

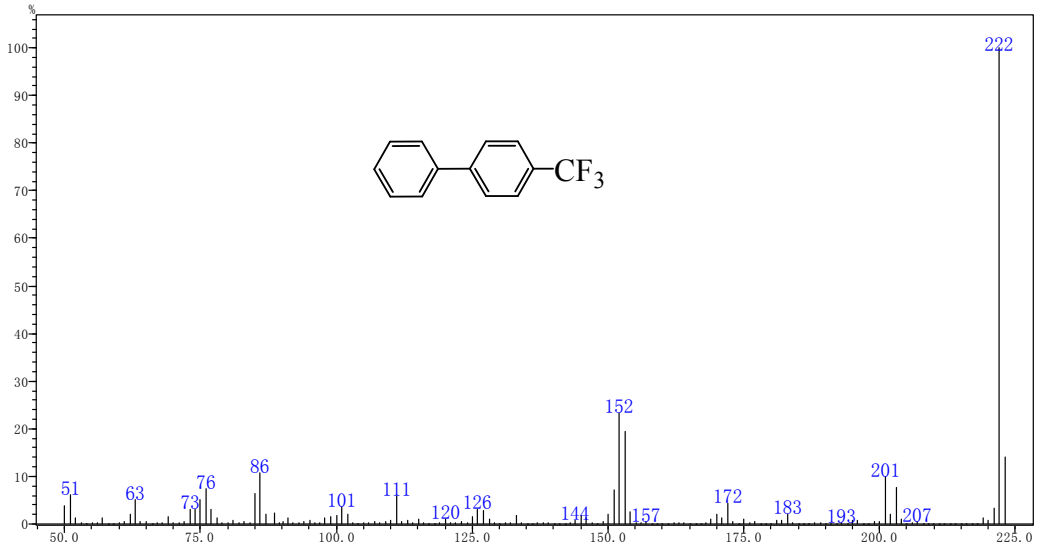

MS (ESI): m/z calcd for M = $C_{13}H_9F_3$: 222.21; found 222 (M).